Recent extensions of the Second RPA method and its applications to soft monopole modes

Danilo Gambacurta
gambacurta@lns.infn.it
INFN-LNS Catania

ADVANCES ON GIANT NUCLEAR MONOPOLE EXCITATIONS AND APPLICATIONS TO MULTI-MESSENGER ASTROPHYSICS
Trento, July 11-15, 2022

Outline

- Theoretical models: RPA and Second RPA (SRPA)
- Improving on the SRPA: the Subtracted SRPA (SSRPA)
- Low-lying dipole excitations in ^{48}Ca: RPA, SRPA and SSRPA vs Data
- Low-lying monopole excitations: soft modes
- Conclusions and Perspectives

Microscopic description of Nuclear Excitations (NEs)

The Random Phase Approximation (RPA)

- The RPA is a widely used approximation for the description of NEs
- Very successful especially within the Energy Density Functional framework (interactions á la Skyrme or Gogny, covariant versions)
- It provides global properties: centroid energies and total strength

However, extensions of the RPA are required for:

- Spreading Width
- Fine Structure and Strength Fragmentation
- Low Lying excitations in closed shell nuclei
- Double exctiations and Anharmonicities, ...

The Second RPA (SRPA): more general excitation operators are introduced

Set of exact eigenstates of the Hamiltonian H

$$H|\nu\rangle = E_\nu \mid \nu\rangle$$

where $\mid 0\rangle$ is the ground state with energy E_0.

Phonon Operators

Let us introduce the operators $Q's$:

$$Q_\nu^\dagger \mid 0\rangle = \mid \nu\rangle, \qquad Q_\nu \mid 0\rangle = 0.$$

Equations of Motion:

$$\langle 0 \mid \left[\delta Q, [H, Q_\nu^\dagger]\right] \mid 0\rangle = \omega_\nu \langle 0 \mid [\delta Q, Q_\nu^\dagger] \mid 0\rangle$$

where

$$\omega_\nu = E_\nu - E_0.$$

Phonon Operators: RPA vs SRPA

Random Phase Approximation (RPA)

$$Q_\nu^\dagger = \underbrace{\sum_{ph} X_{ph}^{(\nu)} \underbrace{a_p^\dagger a_h}_{\text{1p-1h}} - \sum_{ph} Y_{ph}^{(\nu)} \underbrace{a_h^\dagger a_p}_{\text{1h-1p}}}$$

Only Landau Damping, Centroid Energy and Total Strength of GRs

Second Random Phase Approximation (SRPA)

$$Q_\nu^\dagger = \sum_{ph} (X_{ph}^{(\nu)} a_p^\dagger a_h - Y_{ph}^{(\nu)} a_h^\dagger a_p)$$

$$+ \underbrace{\sum_{p_1<p_2, h_1<h_2} (X_{p_1 h_1 p_2 h_2}^{(\nu)} \underbrace{a_{p_1}^\dagger a_{h_1} a_{p_2}^\dagger a_{h_2}}_{\text{2p-2h}} - Y_{p_1 h_1 p_2 h_2}^{(\nu)} \underbrace{a_{h_1}^\dagger a_{p_1} a_{h_2}^\dagger a_{p_2}}_{\text{2h-2p}})}$$

Spreading Width, Fragmentation, Double GRs and Anharmonicites, Low-Lying States

RPA Phonon Operators

$$Q_\nu^\dagger = \sum_{ph} X_{ph}^{(\nu)} a_p^\dagger a_h - \sum_{ph} Y_{ph}^{(\nu)} a_h^\dagger a_p$$

RPA Equations of Motion ($1 \mapsto$ 1p1h)

$$\begin{pmatrix} \mathcal{A}_{11} & \mathcal{B}_{11} \\ -\mathcal{B}_{11}^* & -\mathcal{A}_{11}^* \end{pmatrix} \begin{pmatrix} \mathcal{X}_1^\nu \\ \mathcal{Y}_1^\nu \end{pmatrix} = \omega_\nu \begin{pmatrix} \mathcal{X}_1^\nu \\ \mathcal{Y}_1^\nu \end{pmatrix}$$

SRPA Phonon Operators

$$Q^{\dagger}_{\nu} = \sum_{ph} (X^{(\nu)}_{ph} a^{\dagger}_{p} a_{h} - Y^{(\nu)}_{ph} a^{\dagger}_{h} a_{p})$$

$$+ \sum_{p_1<p_2, h_1<h_2} (X^{(\nu)}_{p_1 h_1 p_2 h_2} a^{\dagger}_{p_1} a_{h_1} a^{\dagger}_{p_2} a_{h_2} - Y^{(\nu)}_{p_1 h_1 p_2 h_2} a^{\dagger}_{h_1} a_{p_1} a^{\dagger}_{h_2} a_{p_2})$$

SRPA Equations of Motion (1$\mapsto$ 1p1h, 2$\mapsto$ 2p2h)

$$\begin{pmatrix} \mathcal{A}_{11} & \mathcal{A}_{12} & \mathcal{B}_{11} & \mathcal{B}_{12} \\ \mathcal{A}_{21} & \mathcal{A}_{22} & \mathcal{B}_{21} & \mathcal{B}_{22} \\ -\mathcal{B}^{*}_{11} & -\mathcal{B}^{*}_{12} & -\mathcal{A}^{*}_{11} & -\mathcal{A}^{*}_{12} \\ -\mathcal{B}^{*}_{21} & -\mathcal{B}^{*}_{22} & -\mathcal{A}^{*}_{21} & -\mathcal{A}^{*}_{22} \end{pmatrix} \begin{pmatrix} \mathcal{X}^{\nu}_{1} \\ \mathcal{X}^{\nu}_{2} \\ \mathcal{Y}^{\nu}_{1} \\ \mathcal{Y}^{\nu}_{2} \end{pmatrix} = \omega_{\nu} \begin{pmatrix} \mathcal{X}^{\nu}_{1} \\ \mathcal{X}^{\nu}_{2} \\ \mathcal{Y}^{\nu}_{1} \\ \mathcal{Y}^{\nu}_{2} \end{pmatrix}$$

SRPA Phonon Operators

$$Q^{\dagger}_{\nu} = \sum_{ph} (X^{(\nu)}_{ph} a^{\dagger}_{p} a_{h} - Y^{(\nu)}_{ph} a^{\dagger}_{h} a_{p})$$

$$+ \sum_{p_1<p_2, h_1<h_2} (X^{(\nu)}_{p_1 h_1 p_2 h_2} a^{\dagger}_{p_1} a_{h_1} a^{\dagger}_{p_2} a_{h_2} - Y^{(\nu)}_{p_1 h_1 p_2 h_2} a^{\dagger}_{h_1} a_{p_1} a^{\dagger}_{h_2} a_{p_2})$$

SRPA Equations of Motion (1$\mapsto$ 1p1h, 2$\mapsto$ 2p2h)

$$\begin{pmatrix} \mathcal{A}_{11} & \mathcal{A}_{12} & \mathcal{B}_{11} & \mathcal{B}_{12} \\ \mathcal{A}_{21} & \mathcal{A}_{22} & \mathcal{B}_{21} & \mathcal{B}_{22} \\ -\mathcal{B}^{*}_{11} & -\mathcal{B}^{*}_{12} & -\mathcal{A}^{*}_{11} & -\mathcal{A}^{*}_{12} \\ -\mathcal{B}^{*}_{21} & -\mathcal{B}^{*}_{22} & -\mathcal{A}^{*}_{21} & -\mathcal{A}^{*}_{22} \end{pmatrix} \begin{pmatrix} \mathcal{X}^{\nu}_{1} \\ \mathcal{X}^{\nu}_{2} \\ \mathcal{Y}^{\nu}_{1} \\ \mathcal{Y}^{\nu}_{2} \end{pmatrix} = \omega_{\nu} \begin{pmatrix} \mathcal{X}^{\nu}_{1} \\ \mathcal{X}^{\nu}_{2} \\ \mathcal{Y}^{\nu}_{1} \\ \mathcal{Y}^{\nu}_{2} \end{pmatrix}$$

Computationally very demanding

- Only recently full large scale SRPA calculations have been performed
- Several applications:
  Pygmy dipole resonance, Giant Resonances (ISGQR, IVGDR, GT, Beta-decay, ...)

RPA Matrices (1p1h configurations)

$$A_{1,1'} = \langle HF \mid \left[a_h^\dagger a_p, [H, a_{p'}^\dagger a_{h'}]\right] \mid HF\rangle$$

$$B_{1,1'} = -\langle HF \mid \left[a_h^\dagger a_p, [H, a_{h'}^\dagger a_{p'}]\right] \mid HF\rangle.$$

SRPA Matrices (1p1h and 2p2h configurations)

$$A_{1,2} = A_{2,1}^* = \left\langle HF\middle|\left[a_h^\dagger a_p, [H, a_{p_1}^\dagger a_{p_2}^\dagger a_{h_1} a_{h_2}]\right]\middle|HF\right\rangle$$

$$A_{2',2} = \left\langle HF\middle|\left[a_{h_2'}^\dagger a_{h_1'}^\dagger a_{p_2'} a_{p_1'}, [H, a_{p_1}^\dagger a_{p_2}^\dagger a_{h_1} a_{h_2}]\right]\middle|HF\right\rangle$$

$$B_{1,2} = B_{2,1}^* = -\left\langle HF\middle|\left[a_p^\dagger a_h, [H, a_{p_1}^\dagger a_{p_2}^\dagger a_{h_1} a_{h_2}]\right]\middle|HF\right\rangle = 0$$

$$B_{2',2} = -\left\langle HF\middle|\left[a_{p_1'}^\dagger a_{p_2'}^\dagger a_{h_1'} a_{h_2'}, [H, a_{p_1}^\dagger a_{p_2}^\dagger a_{h_1} a_{h_2}]\right]\middle|HF\right\rangle = 0$$

Quasi Boson Approximation (QBA) **is still used**

The vacuum of the Q's operators $\mid 0\rangle$ is not known:

$$\mid 0\rangle \mapsto \mid HF\rangle, \qquad \left[a_p^\dagger a_h, a_{h'}^\dagger a_{p'}\right] \approx \delta_{pp'}\delta_{hh'}$$

RPA Matrices (1p-1h configurations)

$$A_{1,1'} \sim \epsilon_{HF} + \langle ph|V|ph\rangle$$

$$B_{1,1'} \sim +\langle pp|V|hh\rangle$$

SRPA Matrices (1p-1h and 2p-2h configurations)

$$A_{1,2} \sim \langle ph|V|pp\rangle + \langle hh|V|hp\rangle$$

$$A_{2',2} \sim \epsilon_{HF} + \langle ph|V|ph\rangle + \langle pp|V|pp\rangle + \langle hh|V|hh\rangle$$

The Subtraction procedure

Large scale SRPA calculations have shown that:

- The SRPA strength distribution is sistematically shifted towards lower energies compared to the RPA one
- This shift is very strong ($\simeq$ 3-4 MeV), RPA description often spoiled

Origins and Causes:

1. Quasi Boson Approximation and stability problems in SRPA
2. Use of effective interactions in beyond-mean field methods

The Subtraction procedure (I. Tselyaev Phys. Rev. C 75, 024306 (2007))

- Designed for beyond RPA approaches
- It restores the Thouless theorem, e.g. instabilities are removed
- Static ($\omega = 0$) limit of the SRPA imposed to be equal to the RPA one

From SRPA to an Energy dependent RPA-like problem

- The SRPA problem as an energy-dependent RPA problem

$$A_{1,1'} \mapsto \tilde{A}_{1,1'}(\omega) = A^{RPA}_{1,1'} + \sum_{2,2'} A_{1,2}(\omega + i\eta - A_{2,2'})^{-1} A_{2',1'} = A^{RPA}_{1,1'} + A^{Cor}_{1,1'}(\omega)$$

The Subtraction procedure

From SRPA to an Energy dependent RPA-like problem

- The SRPA problem as an energy-dependent RPA problem

$$A_{1,1'} \mapsto \tilde{A}_{1,1'}(\omega) = A^{RPA}_{1,1'} + \sum_{2,2'} A_{1,2}(\omega + i\eta - A_{2,2'})^{-1} A_{2',1'} = A^{RPA}_{1,1'} + A^{Cor}_{1,1'}(\omega)$$

The Subtraction procedure is SRPA (SSRPA)

- Subtraction of the zero–frequency limit of the SRPA correction

$$A^{Cor}_{1,1'} \mapsto \tilde{A}^{Cor}_{1,1'}(\omega) = A_{1,1'}(\omega) - A_{1,1'}(\omega = 0) \Rightarrow$$

$$\tilde{A}_{1,1'}(\omega = 0) = A^{RPA}_{1,1'}$$

$$\Rightarrow \Pi^{SSRPA}(\omega = 0) = \Pi^{RPA}$$

The Subtraction procedure

From SRPA to an Energy dependent RPA-like problem

- The SRPA problem as an energy-dependent RPA problem

$$A_{1,1'} \mapsto \tilde{A}_{1,1'}(\omega) = A^{RPA}_{1,1'} + \sum_{2,2'} A_{1,2}(\omega + i\eta - A_{2,2'})^{-1} A_{2',1'} = A^{RPA}_{1,1'} + A^{Cor}_{1,1'}(\omega)$$

The Subtraction procedure is SRPA (SSRPA)

- Subtraction of the zero–frequency limit of the SRPA correction

$$A^{Cor}_{1,1'} \mapsto \tilde{A}^{Cor}_{1,1'}(\omega) = A_{1,1'}(\omega) - A_{1,1'}(\omega = 0) \Rightarrow$$

$$\tilde{A}_{1,1'}(\omega = 0) = A^{RPA}_{1,1'}$$

$$\Rightarrow \Pi^{SSRPA}(\omega = 0) = \Pi^{RPA}$$

Numerical implementation

- Subtraction performed in diagonal approximation, e.g. $A_{2,2'} \approx \delta_{2,2'} A_{2,2}$
- Full subtraction recently performed (GT strength) [a]

[a] DG, M. Grasso, J. Engel, Physical Review Letters 125, 212501 (2020)

Quadrupole Strength Distribution in ^{16}O: RPA, SRPA and SSRPA

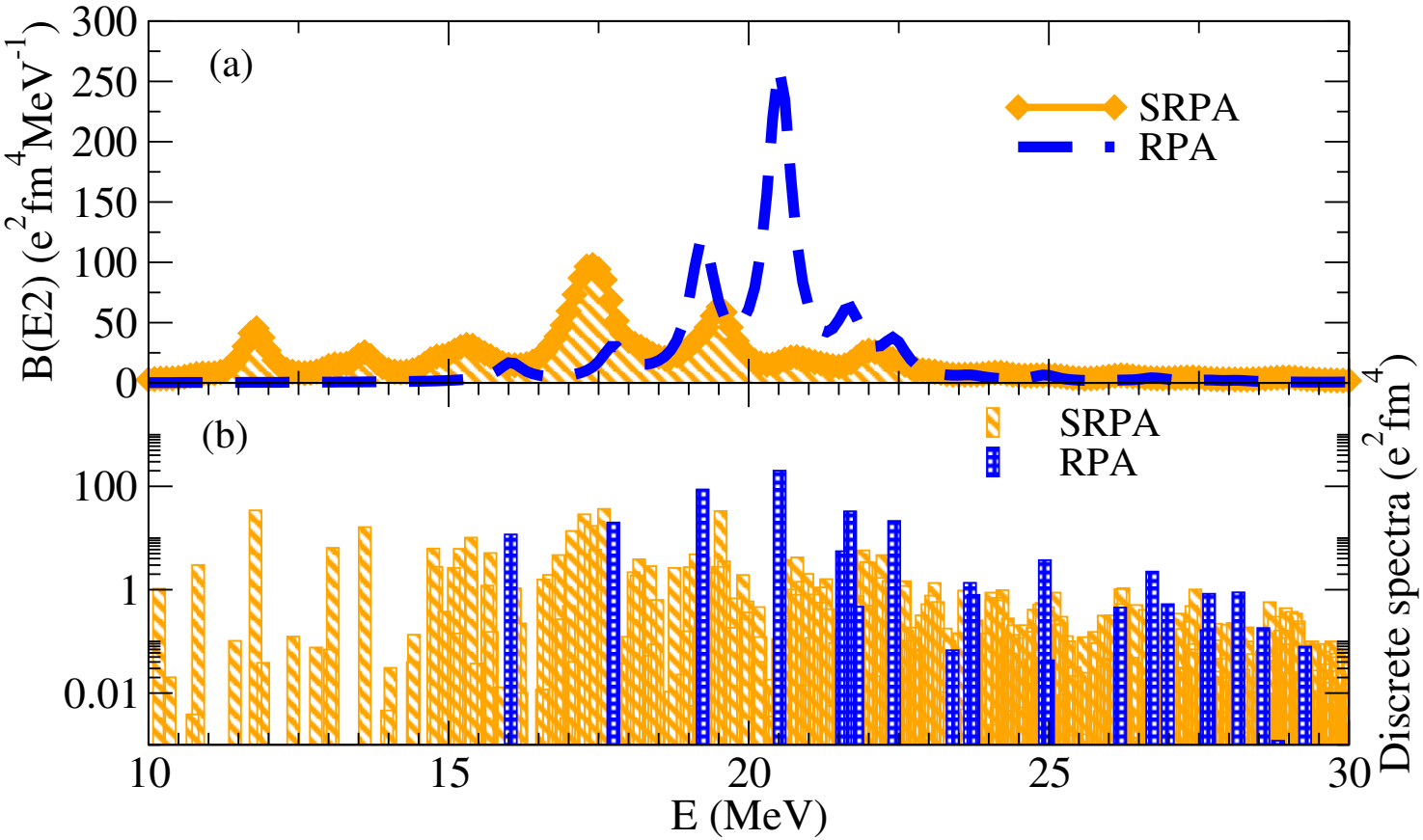

D. G., M. Grasso and J.Engel, Phys. Rev. C 92 , 034303 (2015)

Quadrupole Strength Distribution in ^{16}O: RPA, SRPA and SSRPA

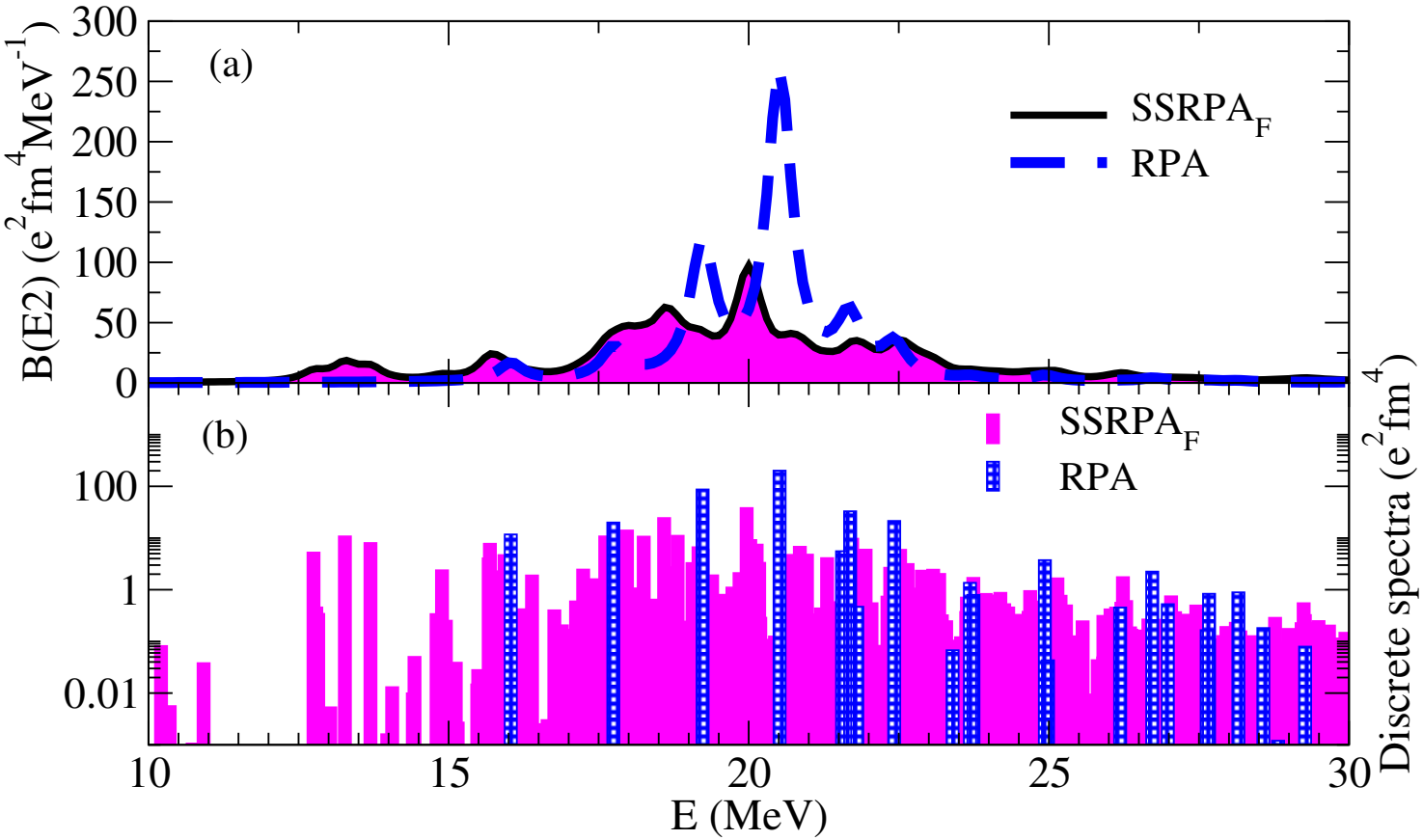

D. G., M. Grasso and J.Engel, Phys. Rev. C 92 , 034303 (2015)

Low-lying dipole response in ^{48}Ca: Motivation

- Experimental low-lying dipole (from 5 to 10 MeV) response in ^{48}Ca stronger than in ^{48}Ca
- Pygmy Dipole Resonance (PDR) type?
- Not described in relativistic and non-relativistic RPA models
- What happens in SRPA [a] ?
- and in the SSRPA [b] ?

[a] D. G. , M. Grasso, and F. Catara, Phys. Rev. C 84, 034301 (2011)
[b] D. G., M. Grasso and O. Vasseur, Physics Letters B 777 (2018) 163–168

Experimental low-lying dipole strength in ^{40},^{48}Ca. (Photon Scattering)

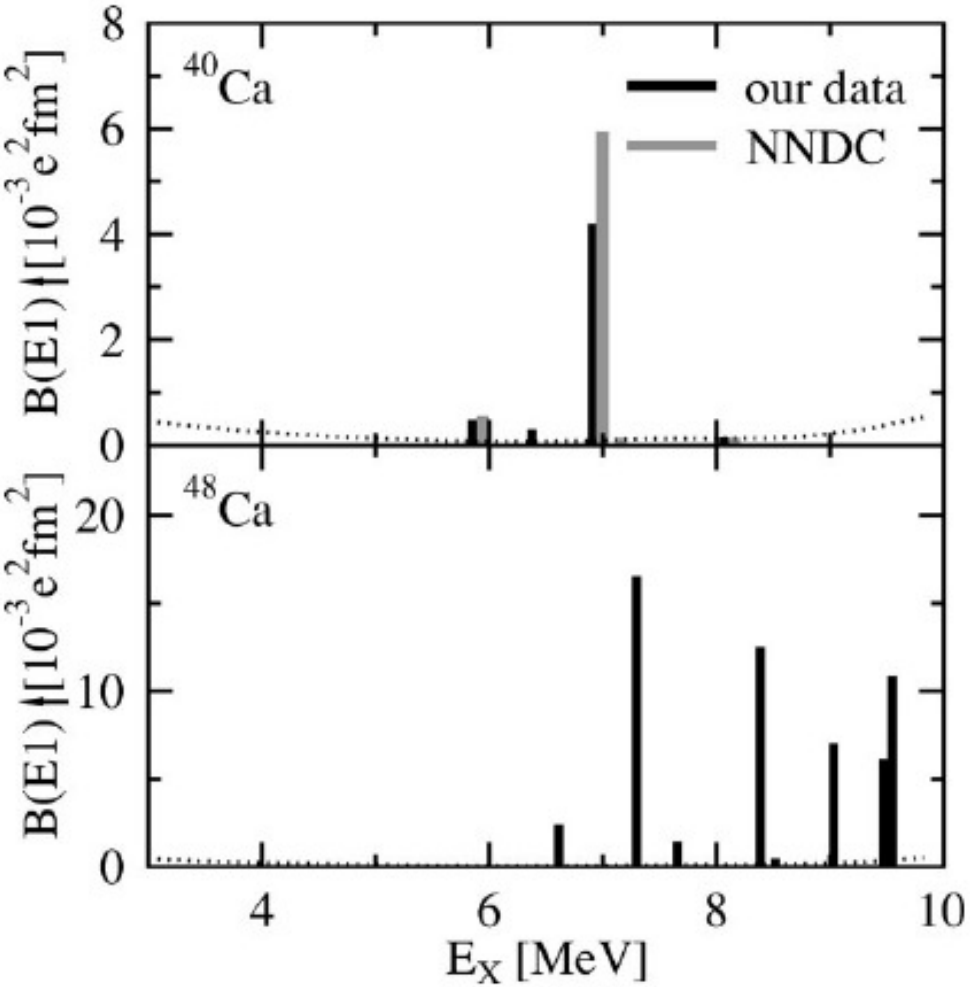

From T. Hartmann *et al.*, PRC 65, 034301, (2002)

$\sum$ B(E1)=5.1 $\pm$ 0.8 ($10^{-3}e^2fm^2$),

Relativistic RPA results

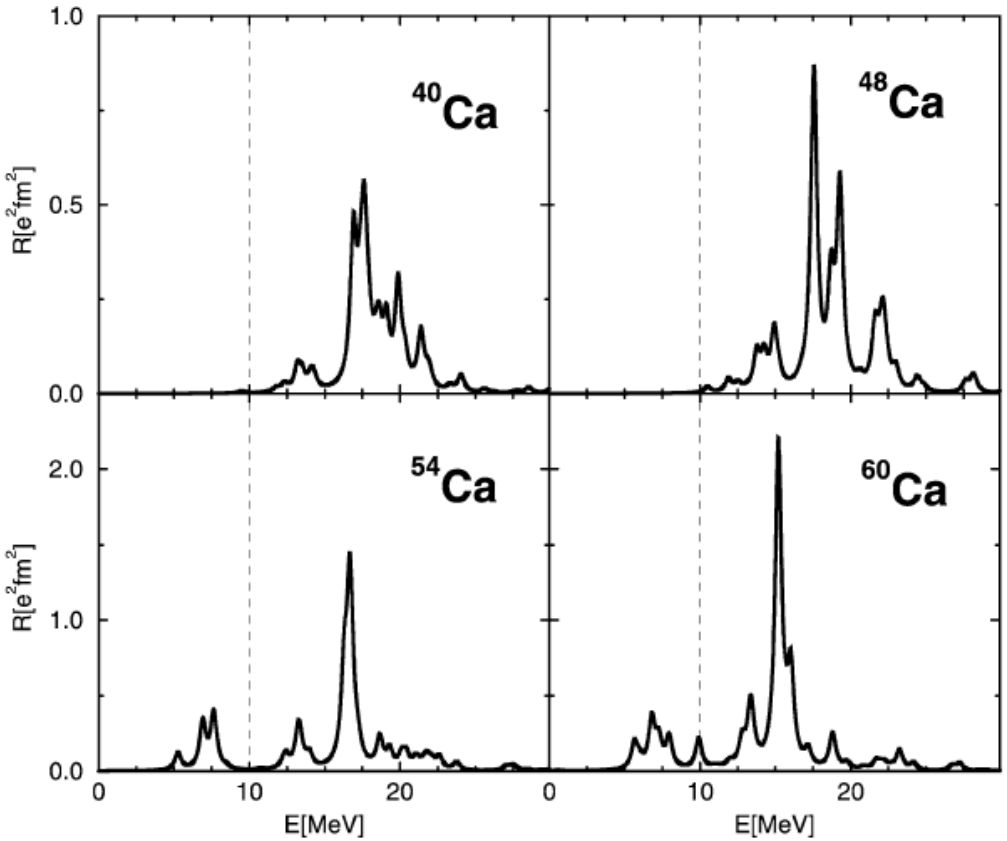

Fig. 5. RRPA isovector dipole strength distributions in Ca isotopes. The thin dashed line tentatively separates the region of giant resonances from the low-energy region below 10 MeV.

From D. Vretenar *et al.*, Nucl. Phys. A 692, 496 (2001)

RPA and SRPA Dipole Strength

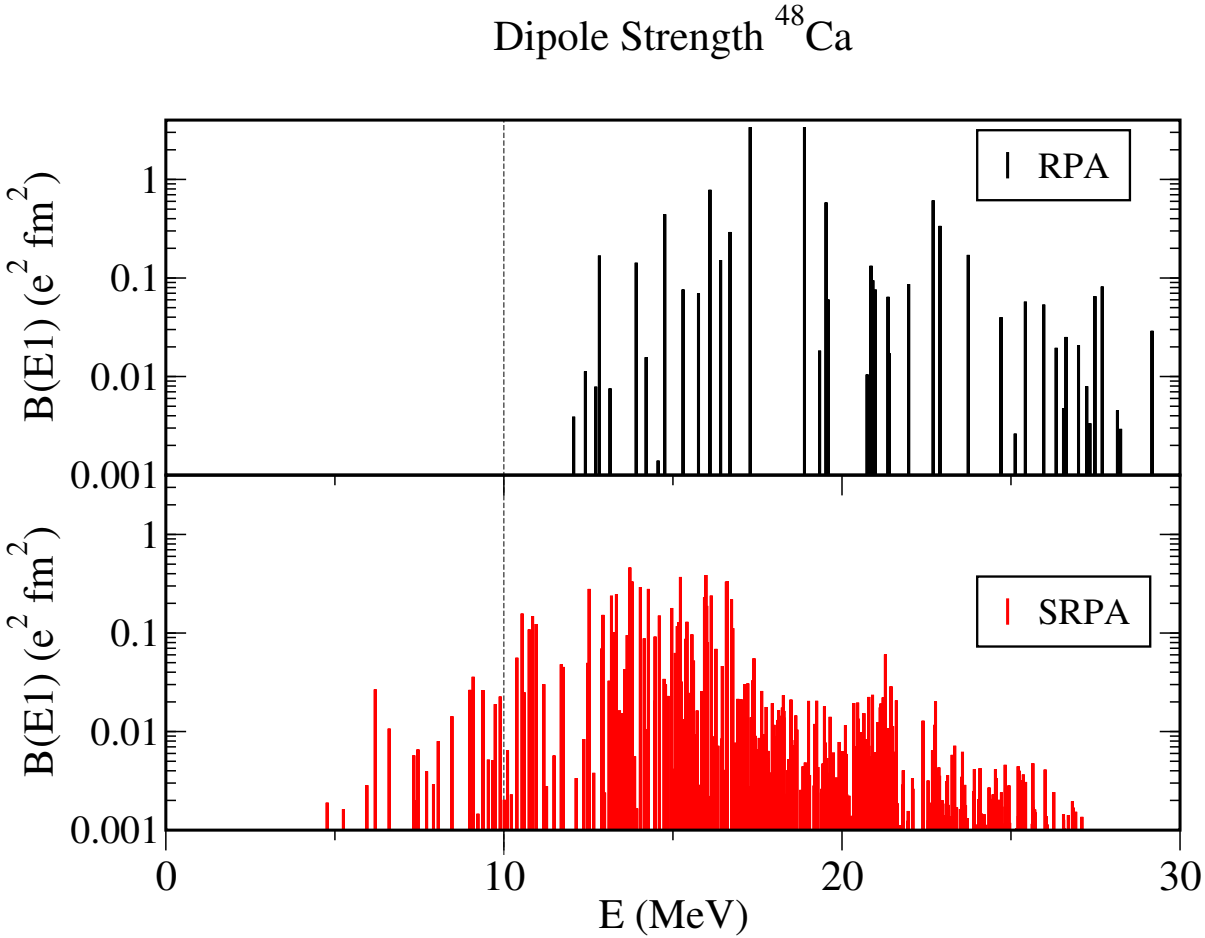

RPA and SRPA Dipole Strength

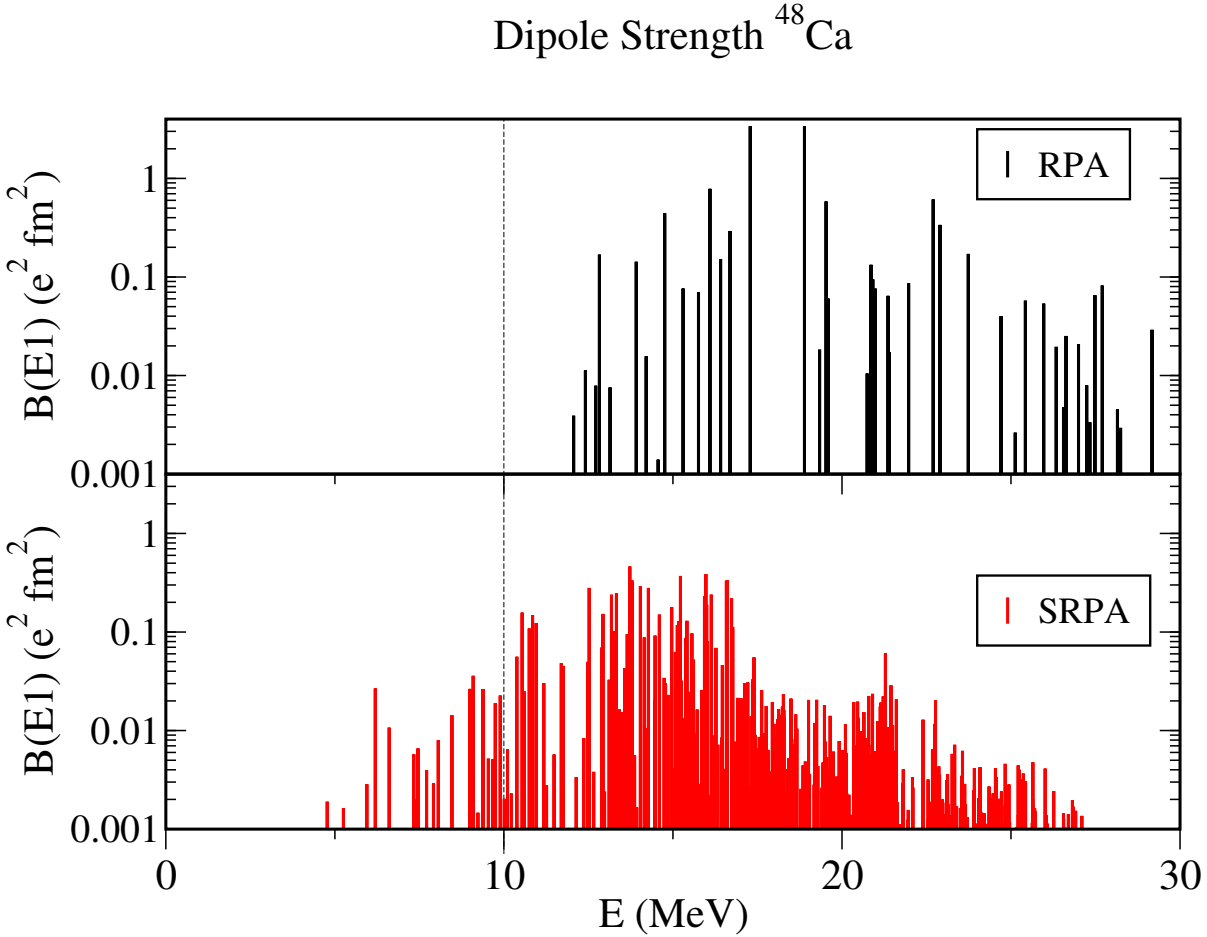

SRPA provides the strength below 10 MeV, but total strength is overestimated.

1p1h and 2p2h contents

$$\langle \nu|\nu\rangle = \sum_{ph}(\mid X^{\nu}_{ph} \mid^2 - \mid Y^{\nu}_{ph} \mid^2) + \sum_{p_1<p_2,h_1<h_2} (\mid X^{\nu}_{p_1h_1p_2h_2} \mid^2 - \mid Y^{\nu}_{p_1h_1p_2h_2} \mid^2)$$

$$= \qquad N_1 \qquad + \qquad N_2 \qquad = 1$$

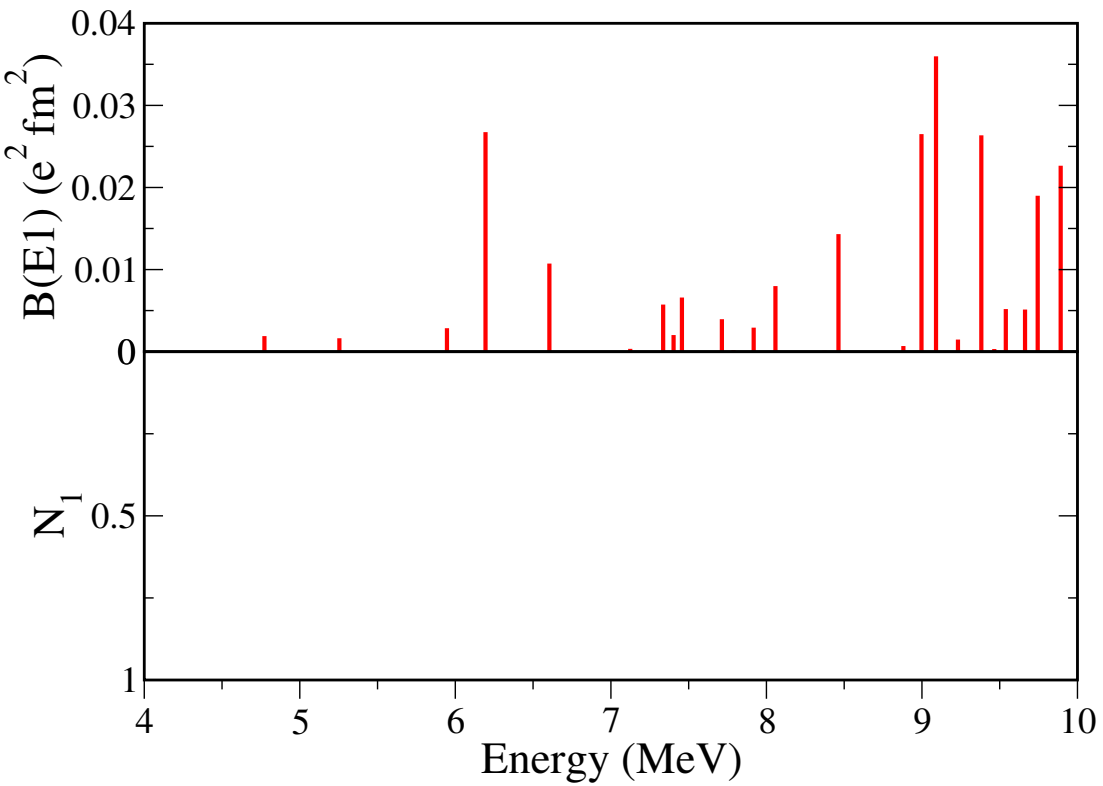

1p1h and 2p2h contents

$$\langle \nu|\nu\rangle = \sum_{ph}(\mid X^{\nu}_{ph} \mid^2 - \mid Y^{\nu}_{ph} \mid^2) + \sum_{p_1<p_2,h_1<h_2} (\mid X^{\nu}_{p_1h_1p_2h_2} \mid^2 - \mid Y^{\nu}_{p_1h_1p_2h_2} \mid^2)$$

$$= \qquad N_1 \qquad + \qquad N_2 \qquad = 1$$

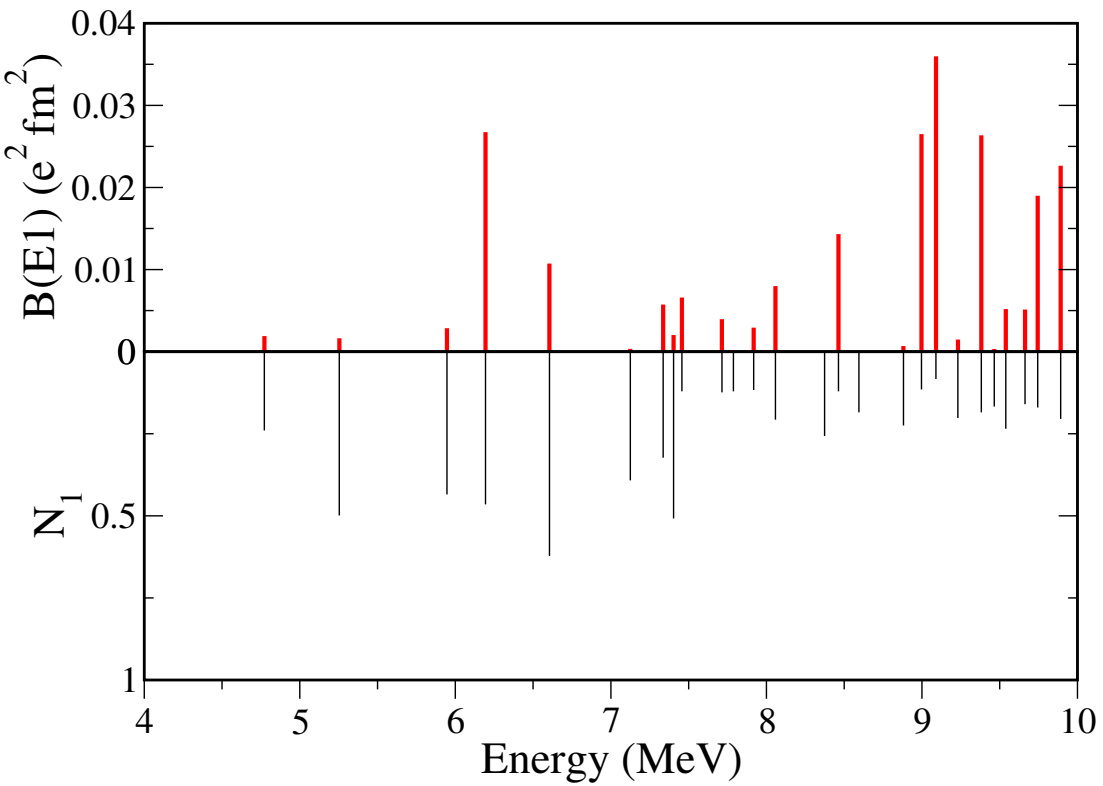

SRPA, SSRPA vs Data

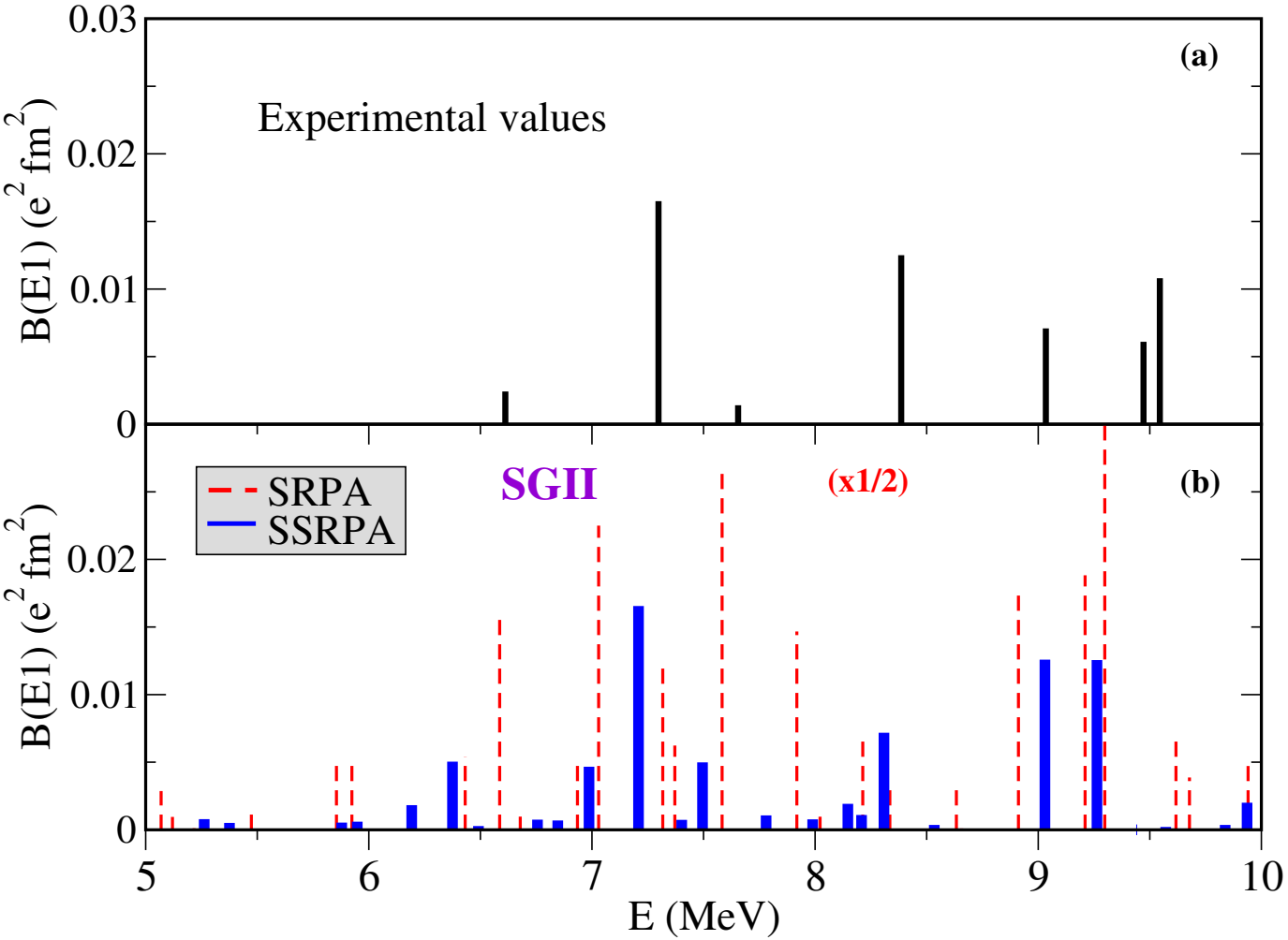

D. Gambacurta , M. Grasso , O. Vasseur, Physics Letters B 777 (2018) 163–168

Total $B(E1)$ and EWSRs (From 5 to 10 MeV)

	Exp	SRPA SGII	SSRPA SGII	SRPA SLy4	SSRPA SLy4
$\sum B(E1)$	0.068 $\pm$ 0.008	0.563	0.078	1.012	0.126
$\sum_i E_i B_i(E1)$	0.570 $\pm$ 0.062	4.618	0.621	8.795	1.062

Experimental and theoretical $\sum B(E1)$ in (e^2 fm^2) and $\sum_i E_i B_i(E1)$ in (MeV e^2 fm^2) summed between 5 and 10 MeV.
From D. G., M. Grasso , O. Vasseur, Physics Letters B 777 (2018) 163–168

Total $B(E1)$ and EWSRs (From 5 to 10 MeV)

	Exp	SRPA SGII	SSRPA SGII	SRPA SLy4	SSRPA SLy4
$\sum B(E1)$	0.068 $\pm$ 0.008	**0.563**	**0.078**	1.012	0.126
$\sum_i E_i B_i(E1)$	0.570 $\pm$ 0.062	**4.618**	**0.621**	8.795	1.062

Experimental and theoretical $\sum B(E1)$ in (e^2 fm^2) and $\sum_i E_i B_i(E1)$ in (MeV e^2 fm^2) summed between 5 and 10 MeV.
From D. G., M. Grasso , O. Vasseur, Physics Letters B 777 (2018) 163–168

Monopole breathing modes in neutron–rich nuclei

The theoretical framework

- We employed the RPA and SSRPA models
- Role of 2p2h configurations
- Excitation energies, transition densities and wave–function components

The key-points of our study

- Soft monopole modes driven by neutron excitations
- Not only at the surface of the nucleus but over its entire volume
- Properties are discussed as a function of the isospin asymmetry
- Possible connection with compressibility of neutron–rich infinite matter (?)
- More details: DG, M. Grasso and O. Sorlin, PRC 100, 014317 (2019)

The nuclei we analysed

- Evolution of the response in Ca isotopes from ^{40}Ca to ^{60}Ca [a]
- $N = 20$ isotones : ^{40}Ca, ^{36}S and ^{34}Si
- The case of ^{68}Ni

[a] Phys. Rev. Lett. 121, (2018) @ RIKEN

Previous studies

- *Dielectric theorem within the Hartree-Fock-Bogoliubov framework* Luigi Capelli, Gianluca Colo and Jun Li, PRC 79, 054329 (2009)
- *Low-energy monopole strength in exotic nickel isotopes* E. Khan, N. Paar and D. Vretenar, PRC 84, 051301(R) (2011)
- *Incompressibility of finite fermionic systems: Stable and exotic atomic nuclei* E. Khan,N. Paar,D. Vretenar,Li-Gang Cao,H. Sagawa and G. Colo',PRC 87, 064311 (2013)
- *Self-consistent Hartree-Fock and RPA Green's function method indicate no pygmy resonance in the monopole response of neutron-rich Ni isotopes* I. Hamamoto and H. Sagawa, PRC 90, 031302(R) (2014)
- *Low-energy monopole strength in spherical and axially deformed nuclei Cluster and soft modes*, F. Mercier, J.-P. Ebran, and E. Khan, Phys. Rev. C 105, 034343 (2022)

Monopole strength distribution in Ca isotopes

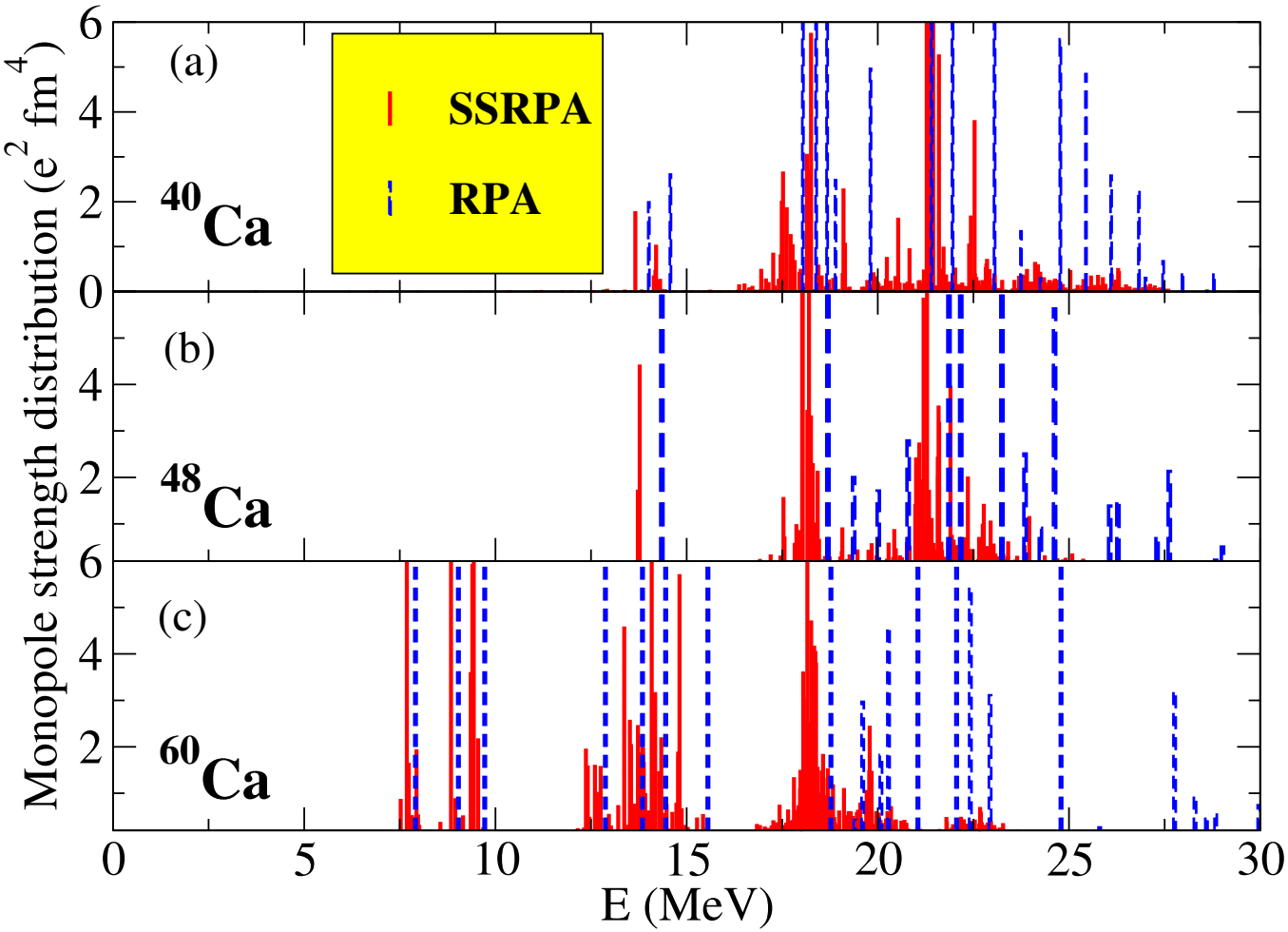

(a) Monopole strength distribution computed with RPA (dashed blue bars) and SSRPA (full red bars) for ^{40}Ca; (b) Same as in (a) but for ^{48}Ca; (c) Same as in (a) but for ^{60}Ca.

Comparison with data from Y.-W. Lui, et al., PRC 83, 044327 (2011)

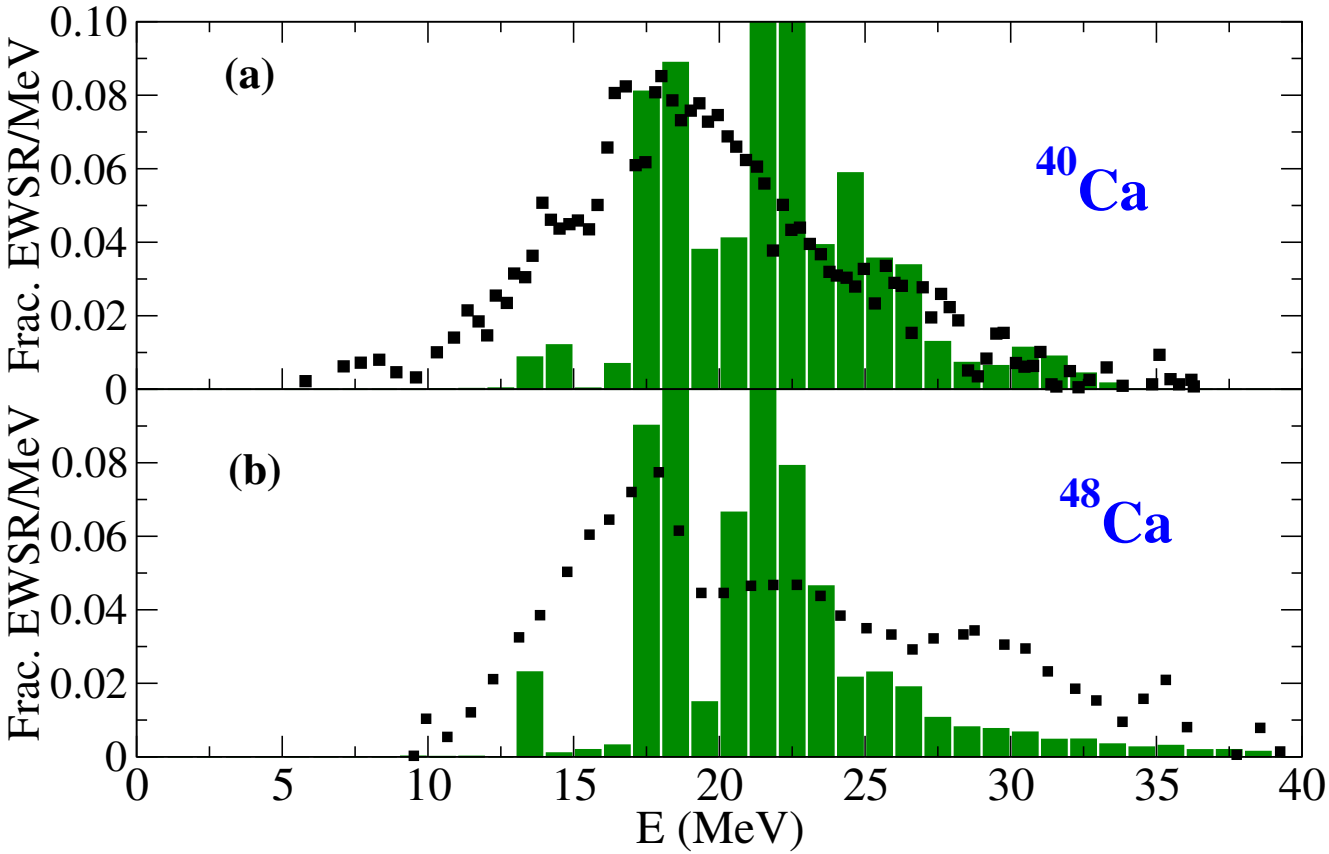

(a) Black squares: experimental results ; green bars: SSRPA predictions for ^{40}Ca; (b) Same as in (a) but for ^{48}Ca.

Comparison with data from Y.-W. Lui, et al., PRC 83, 044327 (2011)

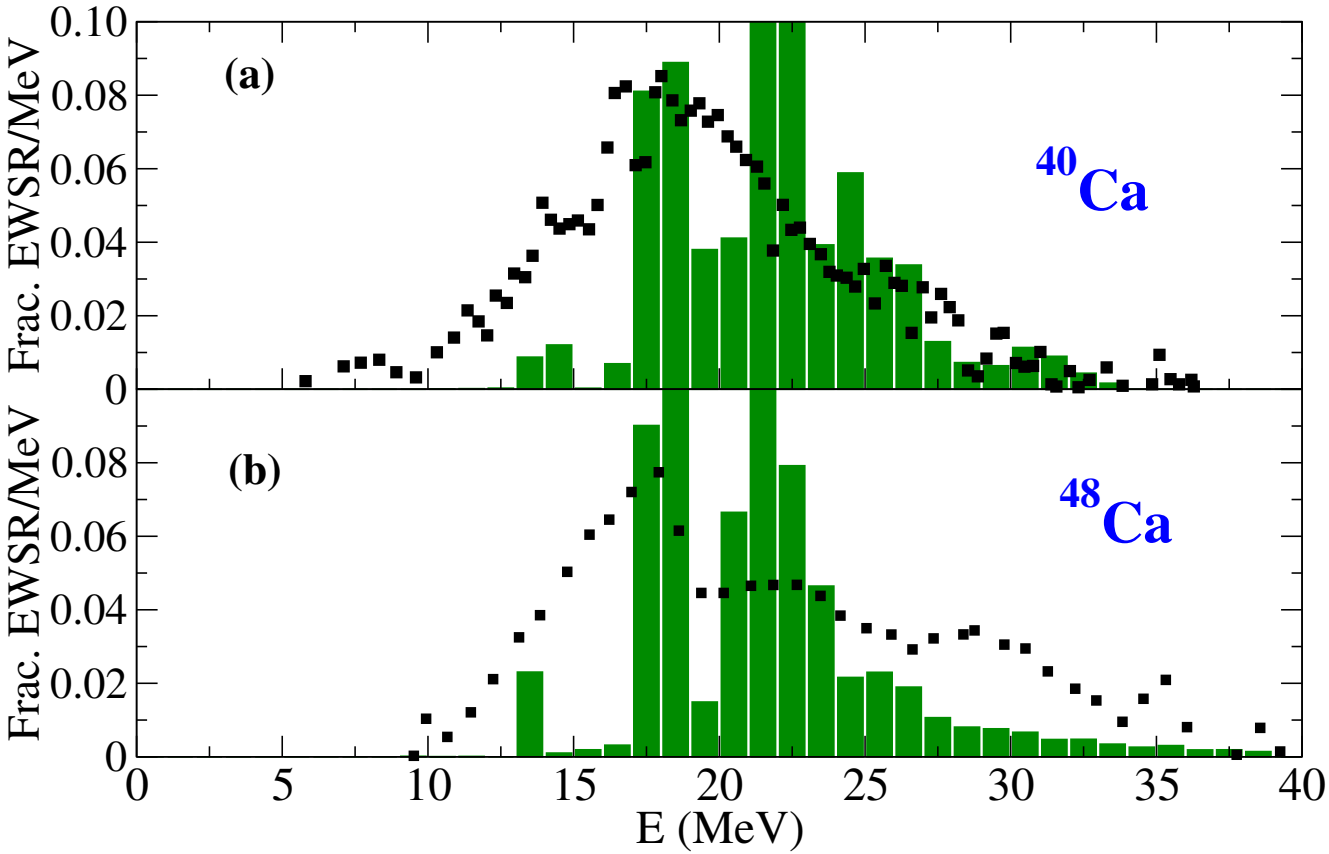

(a) Black squares: experimental results ; green bars: SSRPA predictions for ^{40}Ca; (b) Same as in (a) but for ^{48}Ca.

Centroids (MeV)

^{40}Ca: 21.3 (RPA), 20.7 (SSRPA), 18.3 (Exp)

^{48}Ca: 20.7 (RPA), 20.4 (SSRPA), 19.0 (Exp)

Transition densities in ^{40}Ca

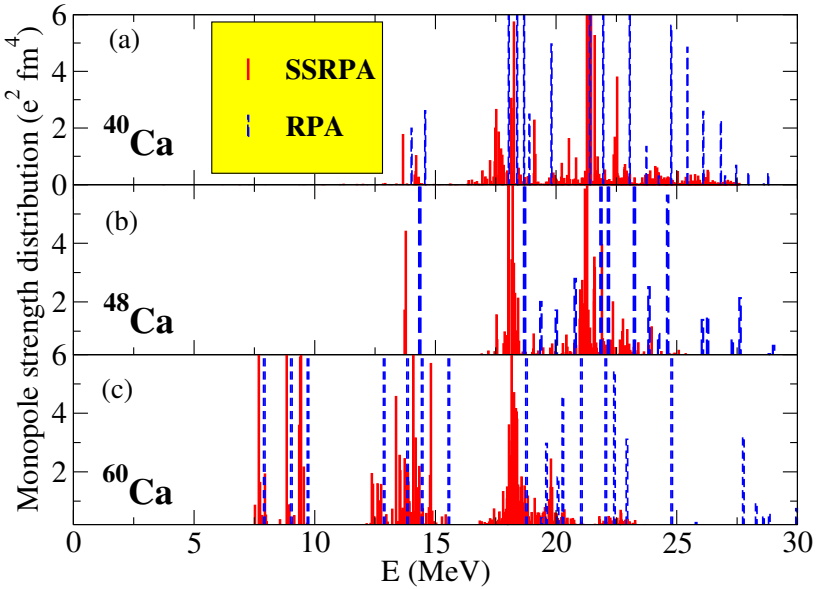

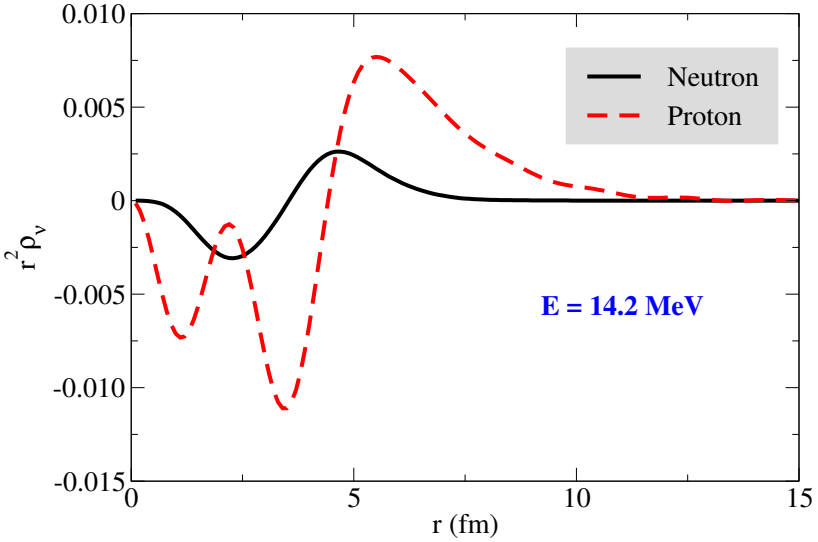

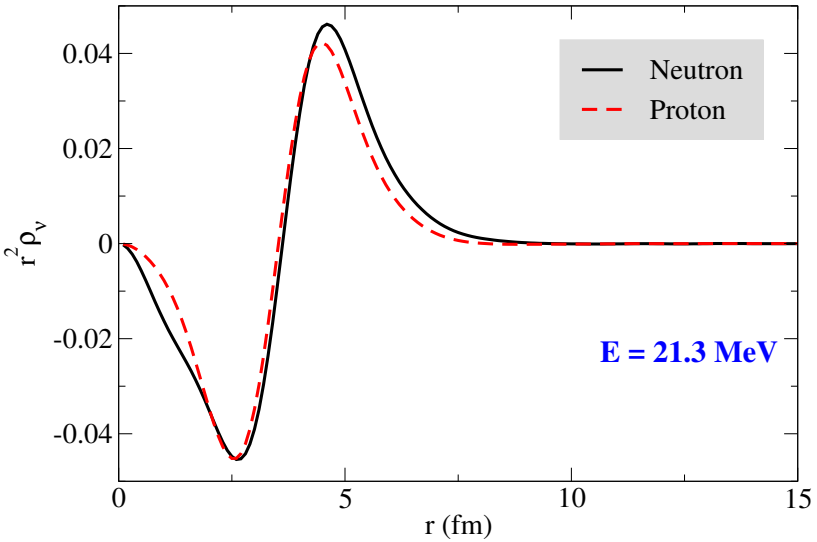

Transition densities in ^{48}Ca

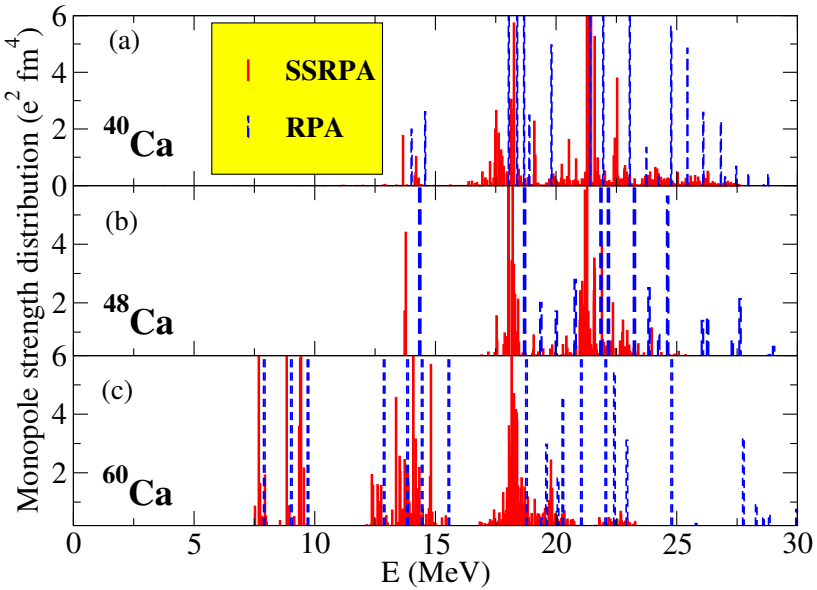

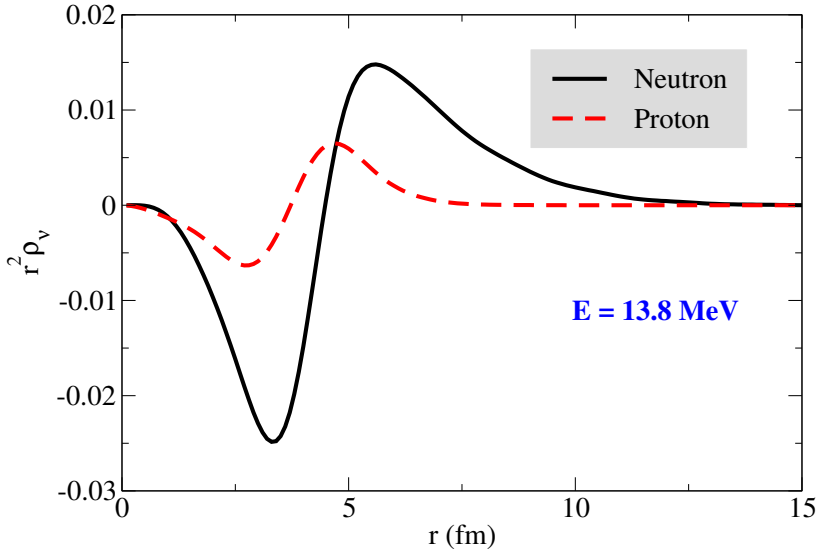

Transition densities in ^{60}Ca

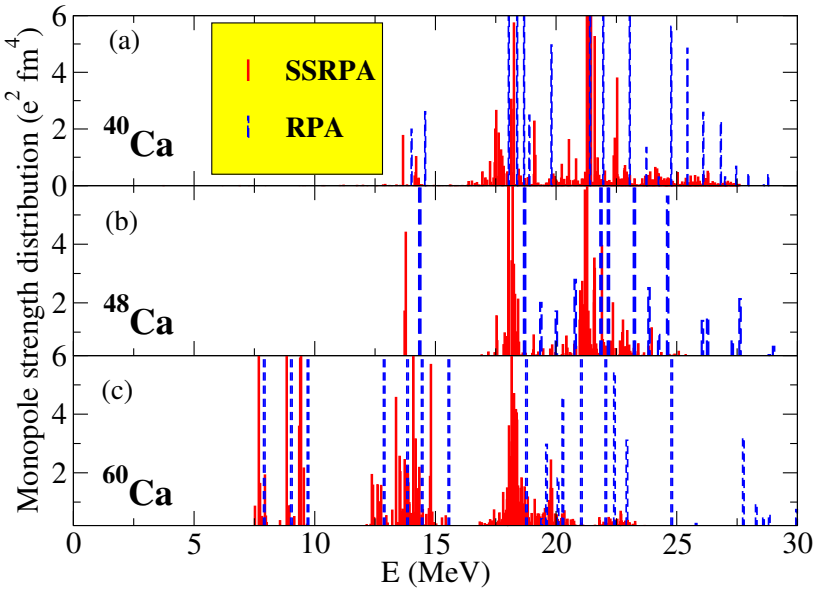

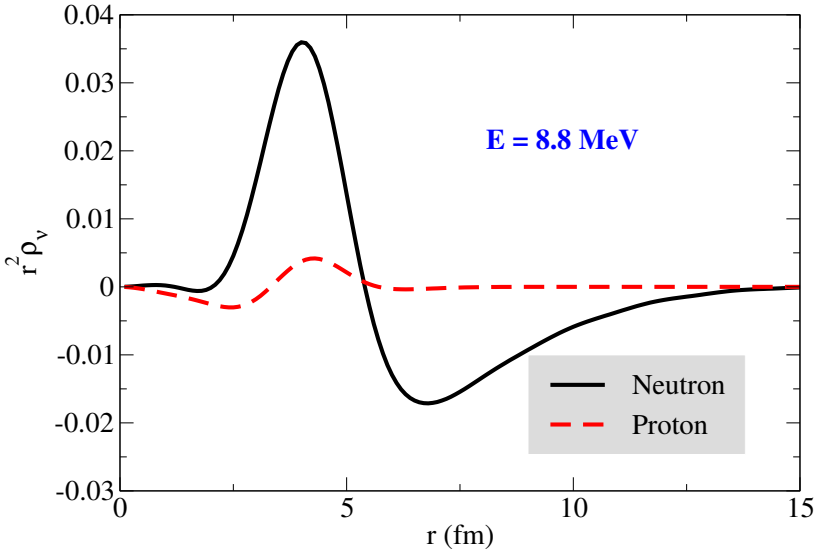

Transition densities in ^{60}Ca

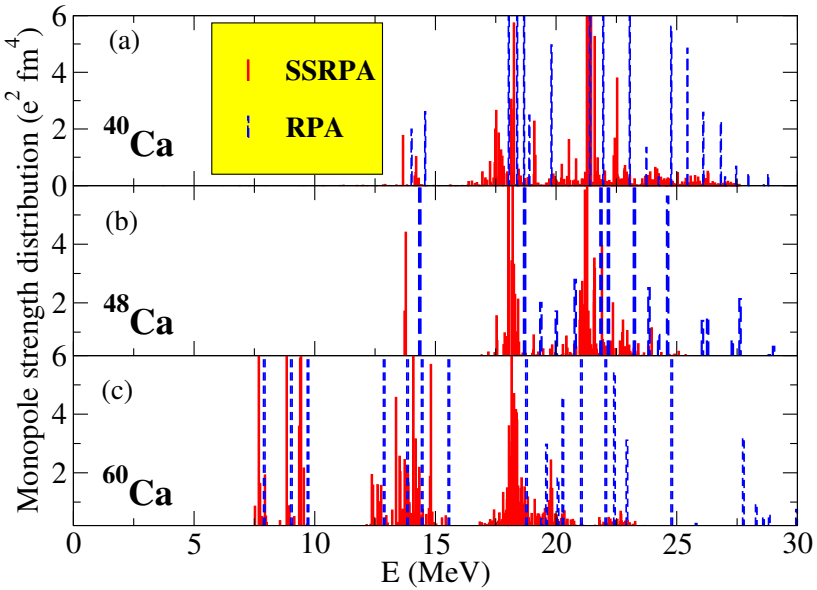

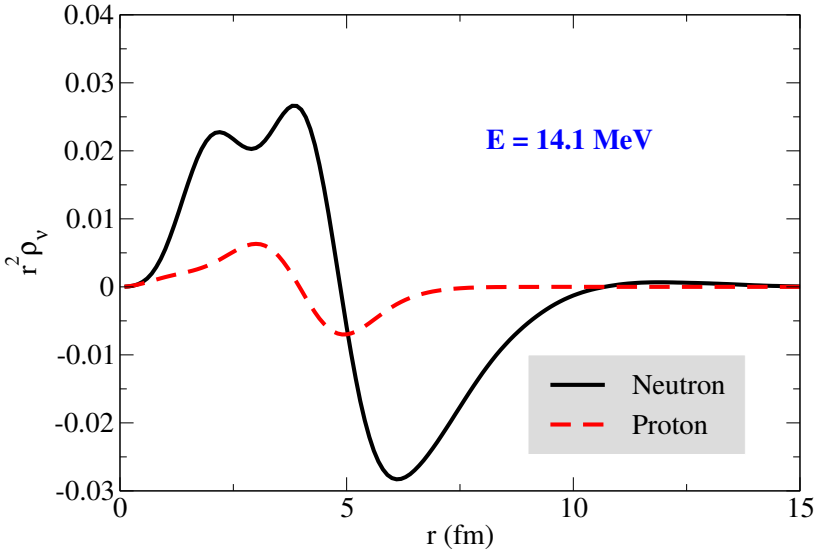

Monopole strength distribution in ^{34}Si and ^{36}S

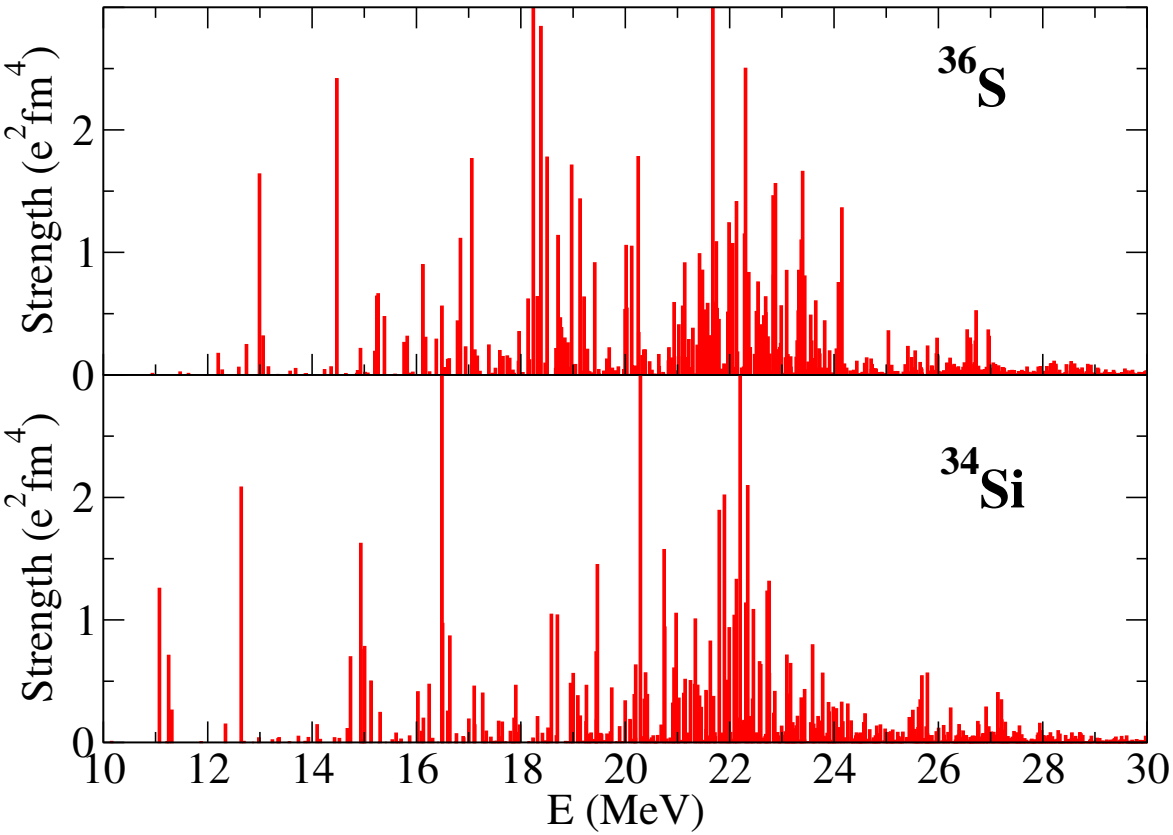

Monopole isoscalar strength distributions calculated for the nuclei ^{36}S (a) and ^{34}Si (b).

Transition densities in ^{34}Si and ^{36}S

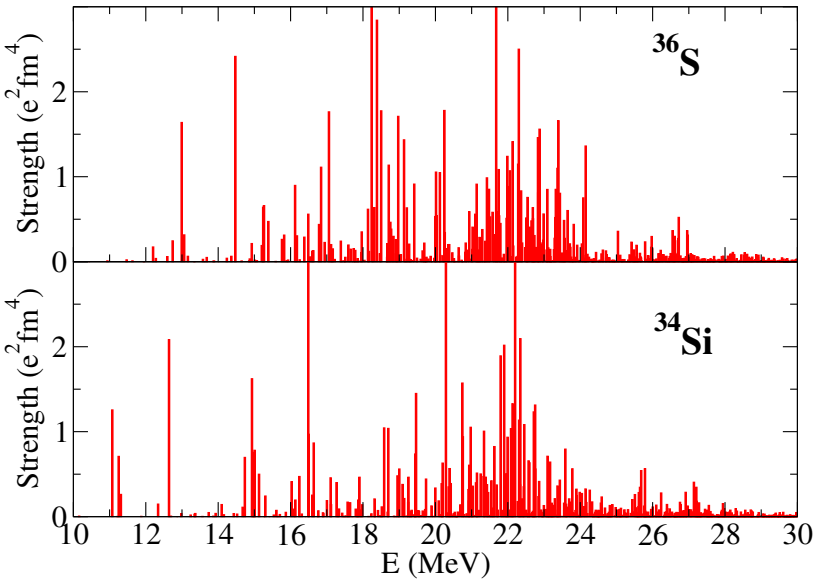

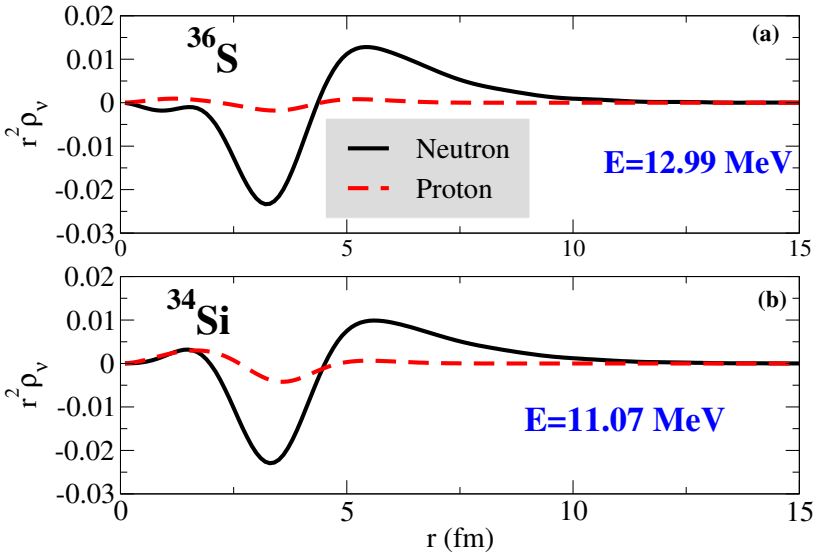

Composition of the peak located at 11.07 (12.99) MeV for ^{34}Si (^{36}S).

^{34}Si	1p1h 54 %	2p2h 46 %
	$[\nu 2d_{3/2}, \nu 1d_{3/2}]^{J=0}$	$[[\pi 3p_{1/2}, \nu 3f_{7/2}]^{J_p=3}[\pi 1d_{5/2}, \nu 2s_{1/2}]^{J_h=3}]^{J=0}$ $[[\pi 4p_{1/2}, \nu 1f_{5/2}]^{J_p=2}[\pi 1d_{5/2}, \nu 2s_{1/2}]^{J_h=2}]^{J=0}$ $[[\pi 4p_{1/2}, \nu 1f_{5/2}]^{J_p=3}[\pi 1d_{5/2}, \nu 2s_{1/2}]^{J_h=3}]^{J=0}$ $[[\pi 6s_{1/2}, \nu 2d_{3/2}]^{J_p=2}[\pi 1d_{5/2}, \nu 1d_{3/2}]^{J_h=2}]^{J=0}$ $[[\pi 6s_{1/2}, \nu 2d_{5/2}]^{J_p=2}[\pi 1d_{5/2}, \nu 1d_{3/2}]^{J_h=2}]^{J=0}$ $[[\pi 3d_{3/2}, \nu 3s_{1/2}]^{J_p=2}[\pi 1d_{5/2}, \nu 1d_{3/2}]^{J_h=2}]^{J=0}$ $[[\pi 3d_{3/2}, \nu 2d_{5/2}]^{J_p=1}[\pi 1d_{5/2}, \nu 1d_{3/2}]^{J_h=1}]^{J=0}$ $[[\pi 3d_{3/2}, \nu 2d_{5/2}]^{J_p=2}[\pi 1d_{5/2}, \nu 1d_{3/2}]^{J_h=2}]^{J=0}$
^{36}S	1p1h 52 %	2p2h 48 %
	$[\nu 2d_{3/2}, \nu 1d_{3/2}]^{J=0}$	$[[\pi 3d_{3/2}, \nu 4d_{3/2}]^{J_p=2}[\pi 1d_{5/2}, \nu 1d_{3/2}]^{J_h=2}]^{J=0}$ $[[\pi 4d_{3/2}, \nu 4s_{1/2}]^{J_p=2}[\pi 2s_{1/2}, \nu 1d_{3/2}]^{J_h=2}]^{J=0}$ $[[\pi 4d_{3/2}, \nu 5s_{1/2}]^{J_p=1}[\pi 2s_{1/2}, \nu 1d_{3/2}]^{J_h=1}]^{J=0}$ $[[\pi 4d_{3/2}, \nu 4d_{3/2}]^{J_p=2}[\pi 2s_{1/2}, \nu 1d_{3/2}]^{J_h=2}]^{J=0}$ $[[\pi 4d_{3/2}, \nu 2d_{5/2}]^{J_p=1}[\pi 2s_{1/2}, \nu 1d_{3/2}]^{J_h=1}]^{J=0}$

Transition densities in ^{68}Ni

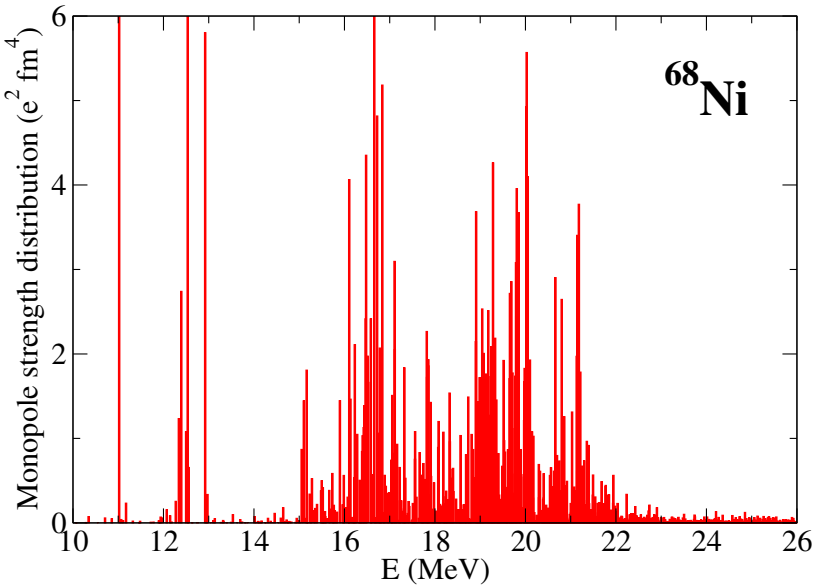

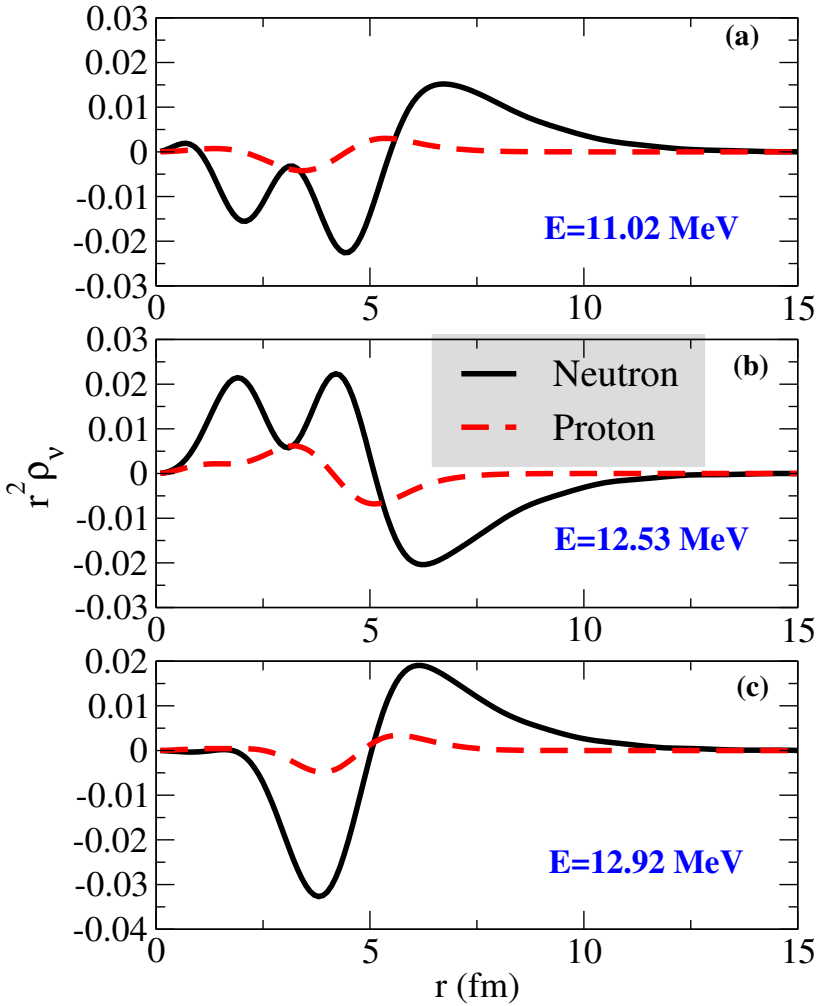

Low–energy states contribution to the EWSR.

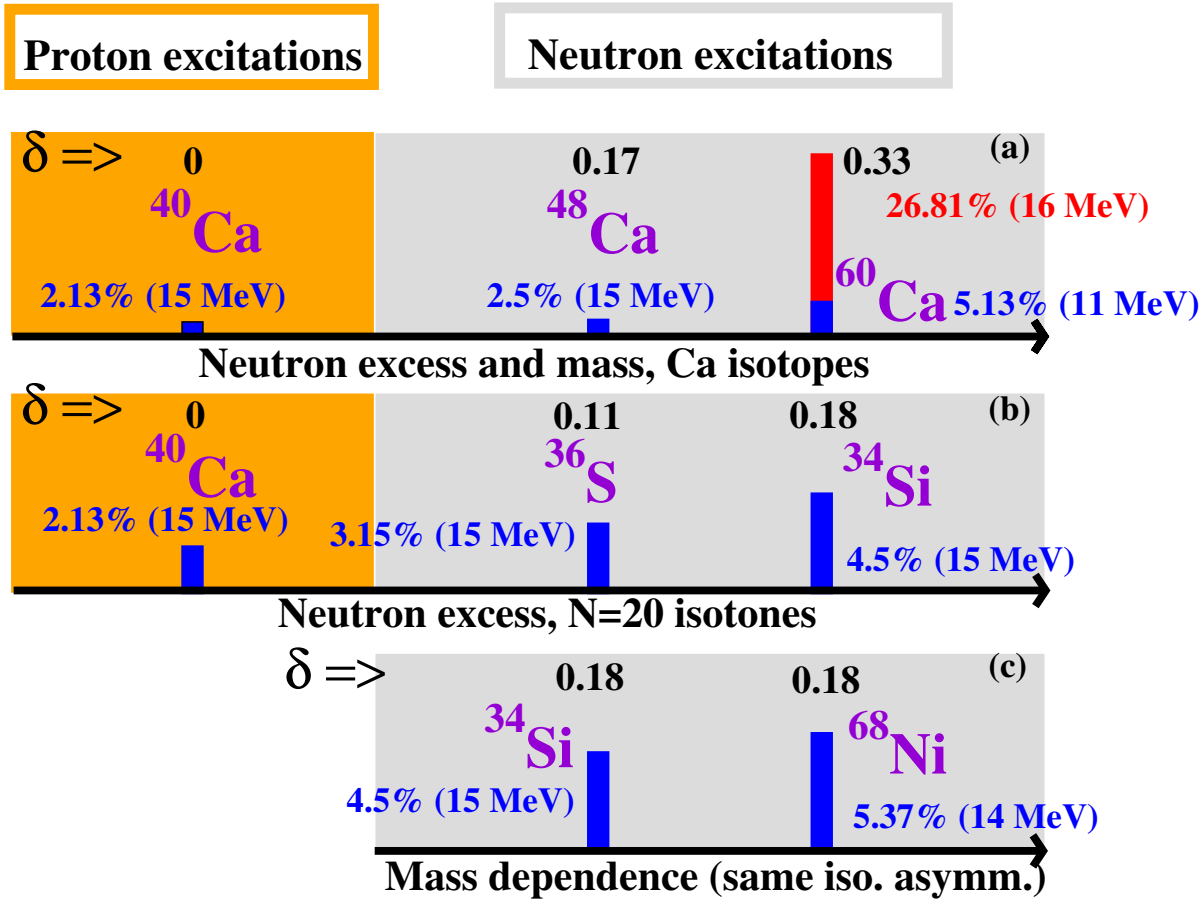

Percentages of the EWSR for several nuclei and corresponding isospin asymmetry δ. (a) Ca isotopes: evolution as a function of the neutron excess and the mass; (b) $N = 20$ isotones: evolution as a function of the neutron excess; (c) Evolution as a function of the mass for two nuclei with the same isospin asymmetry, ^{34}Si and ^{68}Ni.

GMR Centroid and compressibility modulus for symmetric matter

$$E = \sqrt{\frac{\hbar^2\pi^2}{15m}}\sqrt{\frac{K}{\eta_0^2}}, \quad \eta_0 \approx r_0 A^{1/3}, \quad K = 9\rho_0^2\left(\frac{\partial^2 E^{sym}/A}{\partial\rho^2}\right)$$

Nucleus as a liquid drop of a compressibility K, by linerazing the hydrodynamics equations plus boundary conditions[a].

[a] J. P. Blaizot, D. Gogny, and B. Grammaticos, Nucl. Phys. A 265, 315 (1976).

Isospin-asymmetry parameter X and corresponding compressibility K_X

- Link between the isospin asymmetry of neutron–rich matter and the one of the oscillating neutron–rich system involved

$$X_N = 4\pi\int|\rho_\nu^n|r^2dr, \quad X_P = 4\pi\int|\rho_\nu^p|r^2dr$$

  where ρ_ν^n and ρ_ν^p are neutron and proton transition densities, respectively.

- The isospin asymmetry X of a given excited state is $X = \frac{X_N - X_P}{X_N + X_P} \Rightarrow$

$$K_X = 9\rho_{eq}^2\left(\frac{\partial^2 E^X/A}{\partial\rho^2}\right)_{\rho=\rho_{eq}}, \Rightarrow \quad E(X) = \sqrt{\frac{\hbar^2\pi^2}{15m}}\sqrt{\frac{K_X}{\eta_0^2}}$$

Connection with EoS of neutron–rich matter, a qualitative analysis

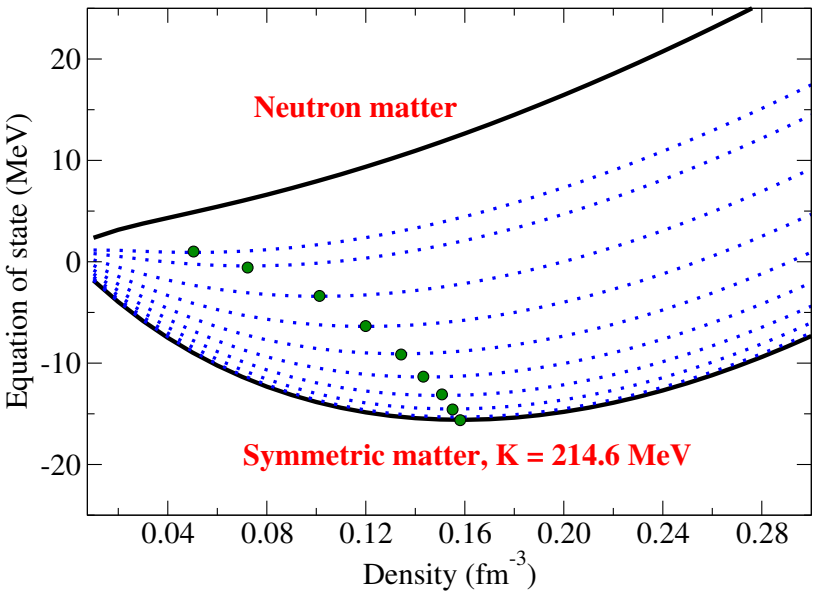

EoS (SGII) from symmetric to pure neutron matter and different asymmetry values X (dotted-lines).
The equilibrium points are represented by green circles for each EoS.

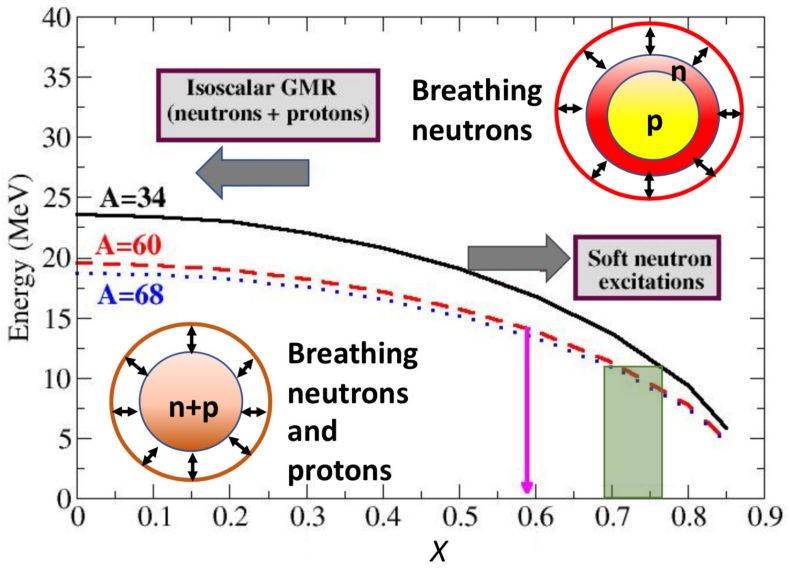

Energy versus the asymmetry value X. Green area represents excitations located at 8.8 (^{60}Ca), 11.07 (^{34}Si), and 11.02 (^{68}Ni) MeV. The magenta arrow indicates the peak located at 14.1 MeV for ^{60}Ca.

Connection with EoS of neutron–rich matter, a qualitative analysis

Nucleus	E (MeV)	X
^{34}Si	11.07	0.73
^{68}Ni	11.02	0.78
^{60}Ca	8.8	0.84
^{60}Ca	14.1	0.73

Microscopic SSRPA X values

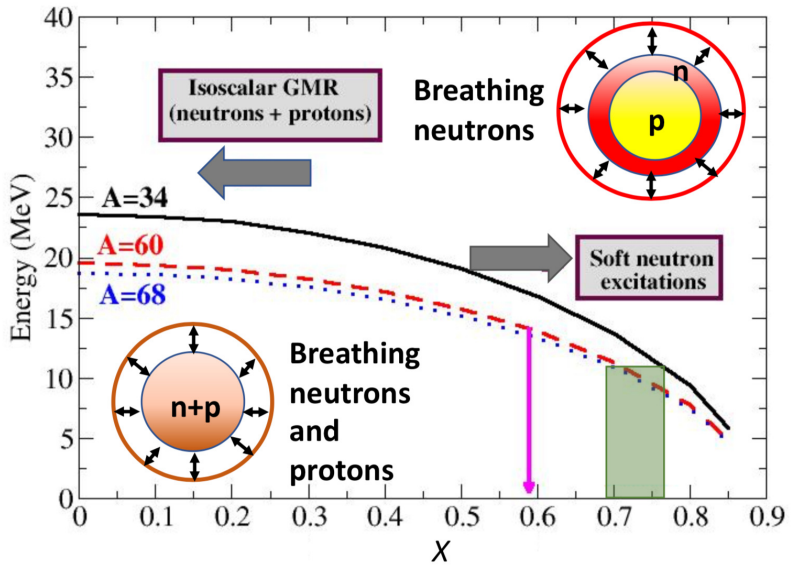

Energy versus the asymmetry value X. Green area represents excitations located at 8.8 (^{60}Ca), 11.07 (^{34}Si), and 11.021 (^{68}Ni) MeV. The magenta arrow indicates the peak located at 14.1 MeV for ^{60}Ca.

Conclusions

- Soft monopole excitations within the beyond–mean–field SSRPA model
- Predicted in both RPA and SSRPA
- The SSRPA modes are slightly shifted to lower energies with higher fragmentation
- Different nuclei to study the mass and neutron excess dependencies
- Appearance of "neutron-driven" excitations in neutron–rich systems, extending in the entire volume
- Qualitative link between their excitation energies and compressibility modulus of neutron–rich matter ... (but) a more robust analysis is needed

Perspectives

- DWBA calculations for soft monopole states (in progress, in collaboration with M. Dupuis, O. Sorlin, M. Vandebrouck, M. Grasso)
- SSRPA calculations for the GMR, effect of 2p2h configurations (Centroid Eneryg and Spreading Width)

Thanks For Your Attention !!!

Backup Slides

SSRPA vs Data, GDR case

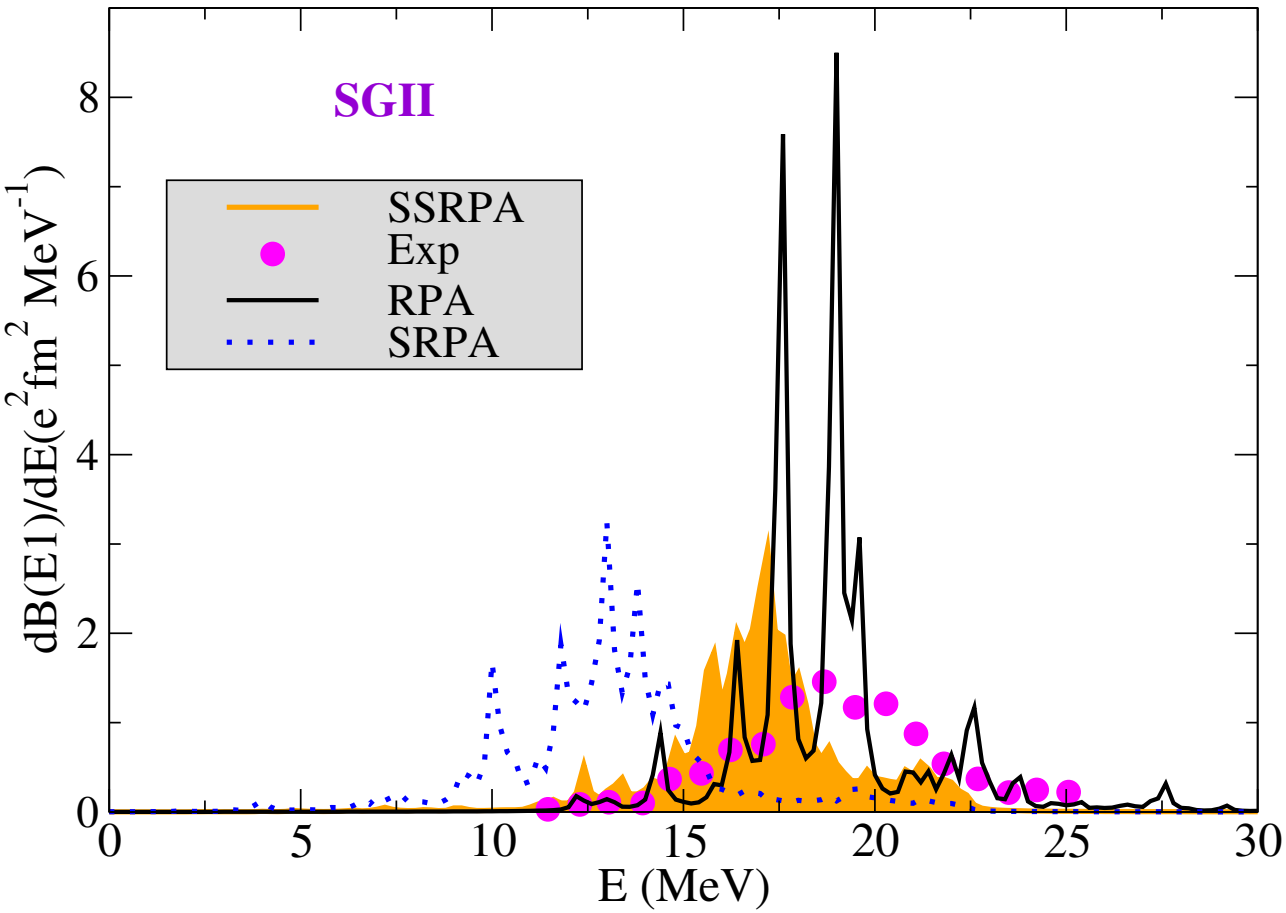

Data From J. Birkhan *et al.*, Phys. Rev. Lett. 118, 252501 (2017);
Theoretical results folded with a Lorentzian having a width of 0.25 MeV
D. G., M. Grasso , O. Vasseur, Physics Letters B 777 (2018) 163–168

SSRPA vs Data, GDR case

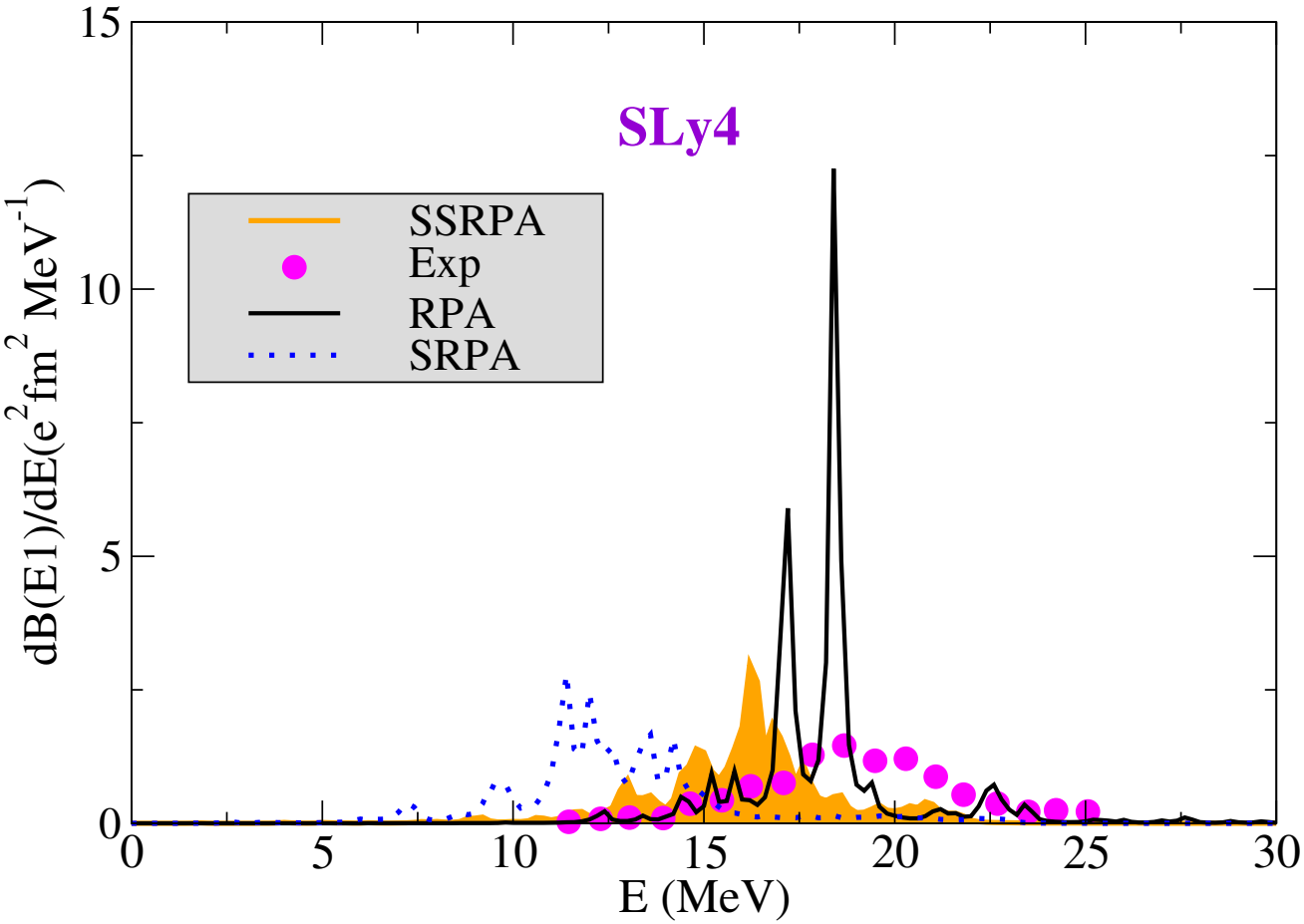

Data From J. Birkhan *et al.*, Phys. Rev. Lett. 118, 252501 (2017);
Theoretical results folded with a Lorentzian having a width of 0.25 MeV
D. G., M. Grasso , O. Vasseur, Physics Letters B 777 (2018) 163–168

SSRPA vs Data, GDR case

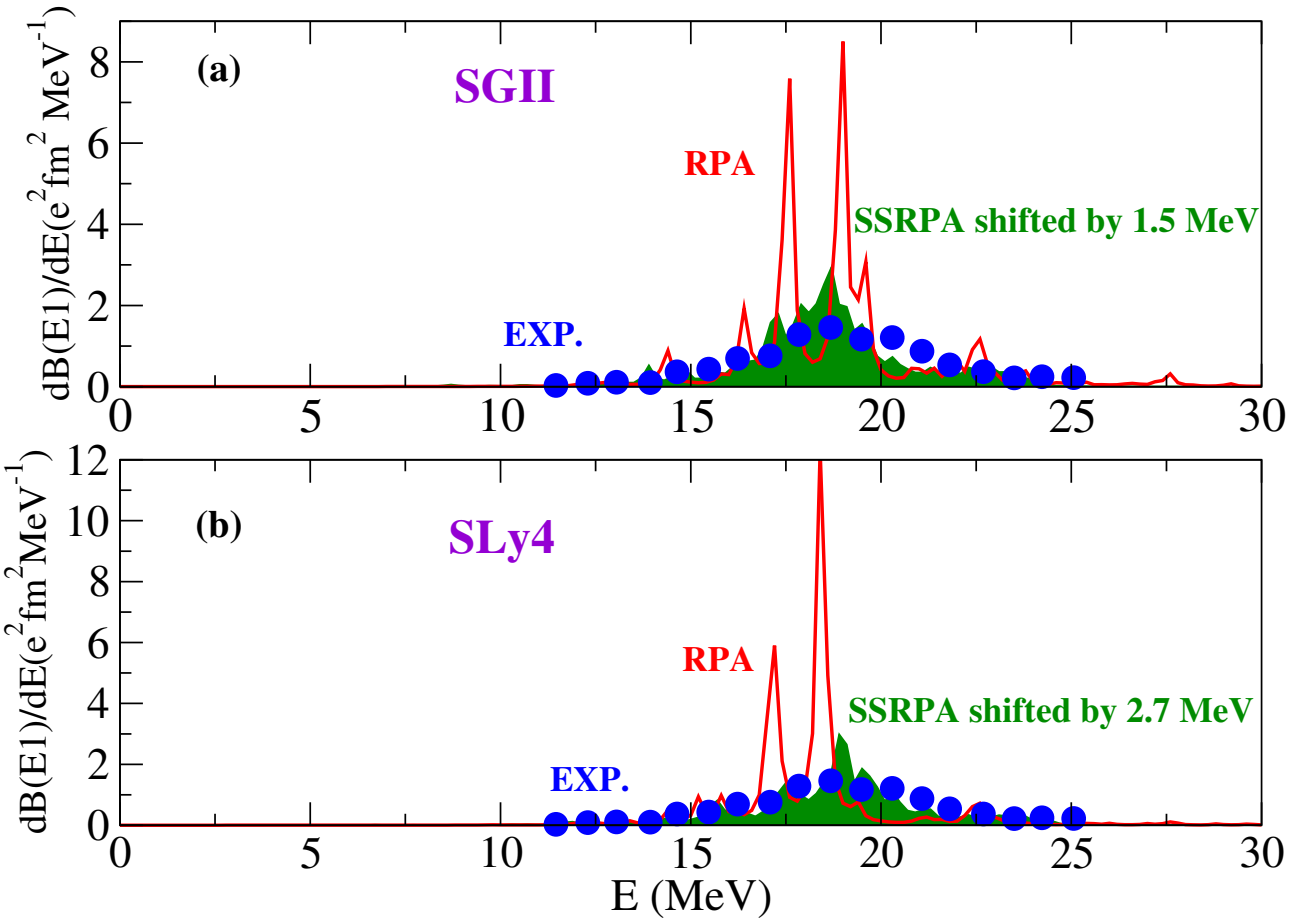

Data From J. Birkhan *et al.*, Phys. Rev. Lett. 118, 252501 (2017);
Theoretical results folded with a Lorentzian having a width of 0.25 MeV
D. G., M. Grasso , O. Vasseur, Physics Letters B 777 (2018) 163–168

Numerical complexity: different approximations schemes

Numerical complexity

- The most demanding task is related to the treatment of the $A_{22'}$ matrix
- The number of 2p-2h configurations can be very large$\simeq 10^7, 10^8$
- We need to calculate the "full" spectrum
- Most demanding tasks:
  a) subtraction procedure, $A_{22'}$ inversion
  b) diagonalization of the SSRPA eigenvalue problem
- Strong simplification if $A_{22'}$ is assumed to be diagonal

Different calculation scheme:

1. SSRPADD: $A_{22'}$ is Diagonal both in a) and b)
2. SSRPADF: $A_{22'}$ is Diagonal both in a) and Full in b)
3. SSRPAFF: $A_{22'}$ is Full both in a) and in b)

GT$^-$ Strength Distribution ^{48}Ca SSRPA results

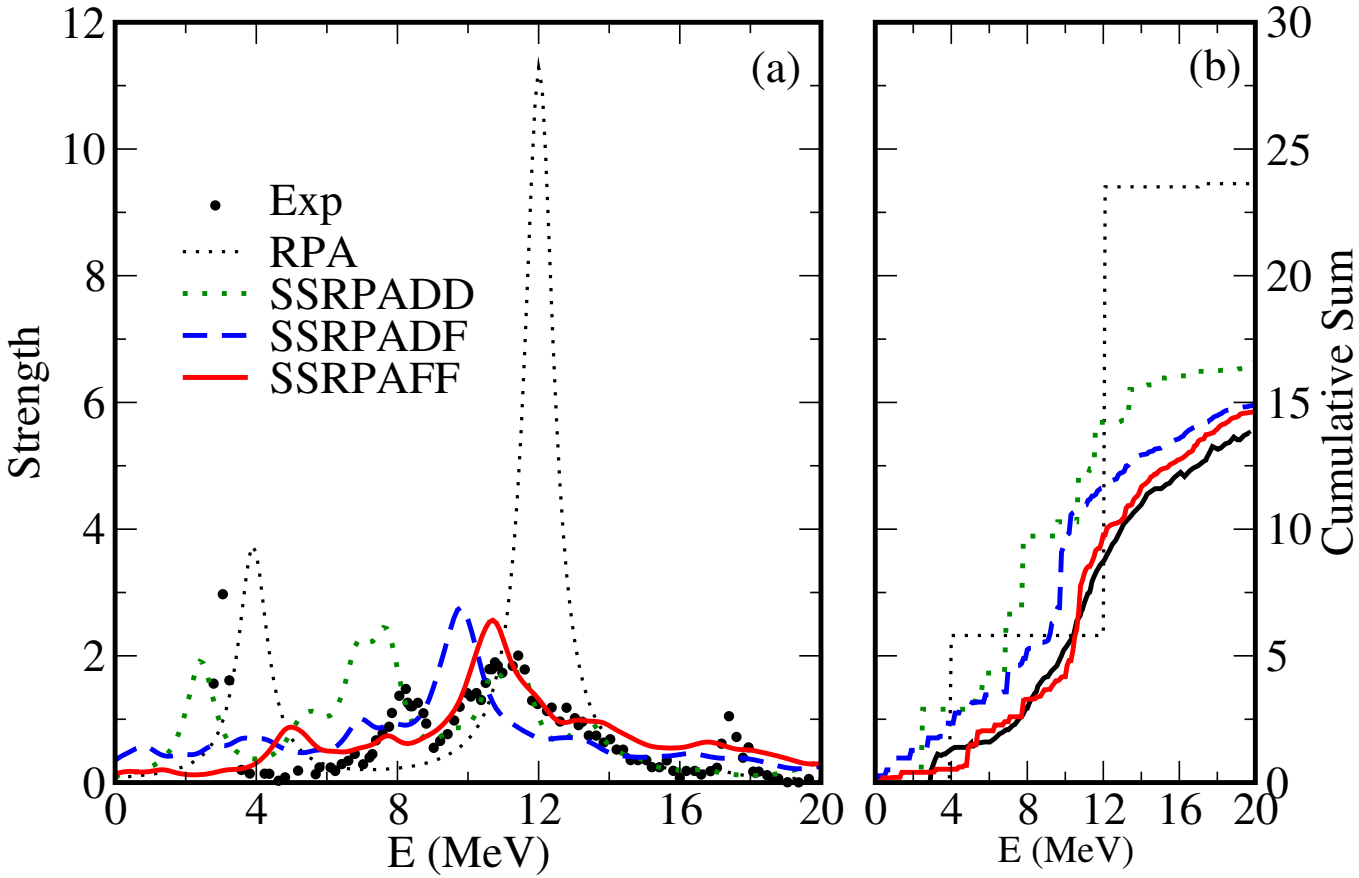

Comparison between SSRPADD, SSRPADF and SSRPAFF results .

From D.Gambacurta and M. Grasso, Phys. Rev. C 105, 014321, (2022)
See also D.Gambacurta, M. Grasso, J. Engel, PRL 125, 212501 (2020)

Systematic calculations for Isoscalar GQRs: from 30Si to 208Pb
Centroid energy

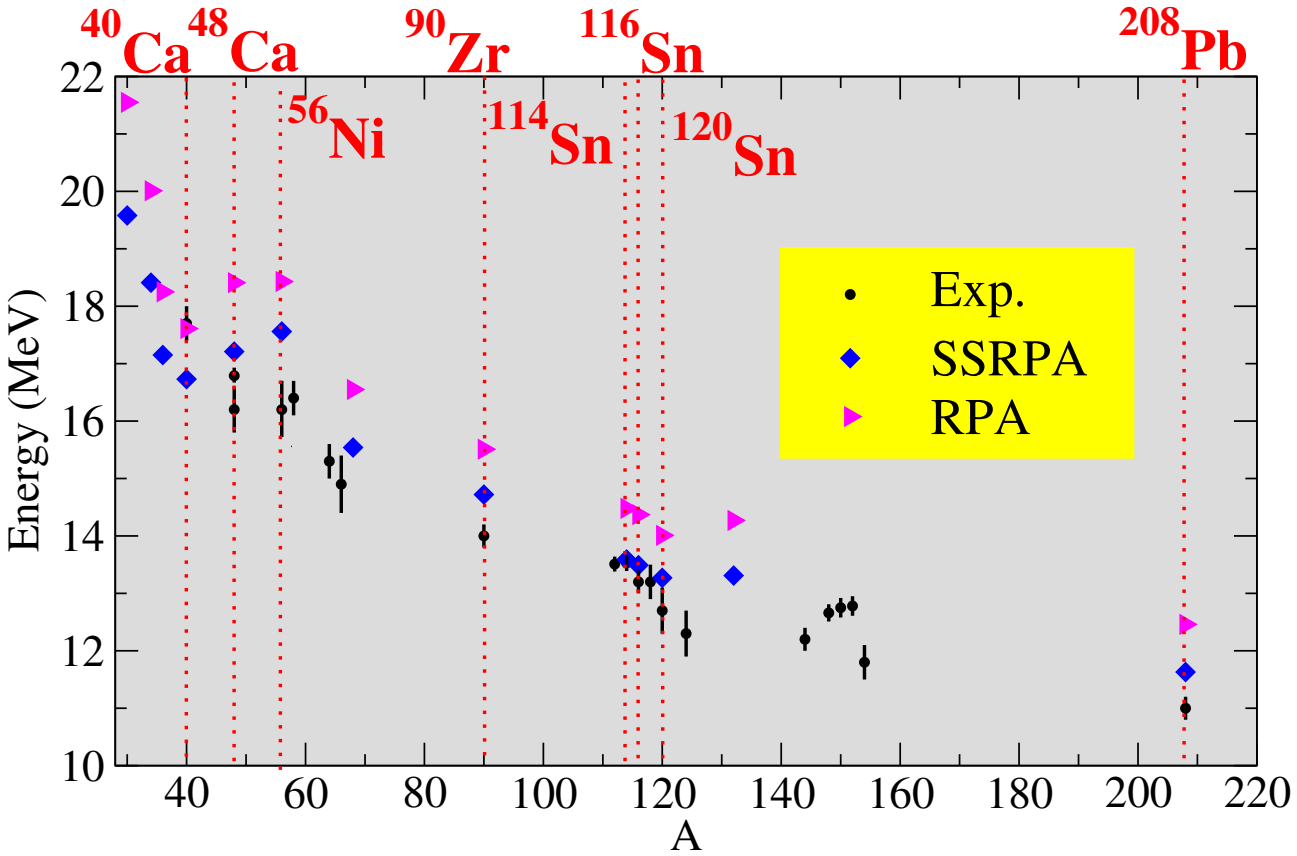

Globally: better agreement with the experimental data compared to RPA
Vasseur, Gambacurta, Grasso, PRC 98, 044313 (2018)

Systematic calculations for Isoscalar GQRs: from 30Si to 208Pb
Width

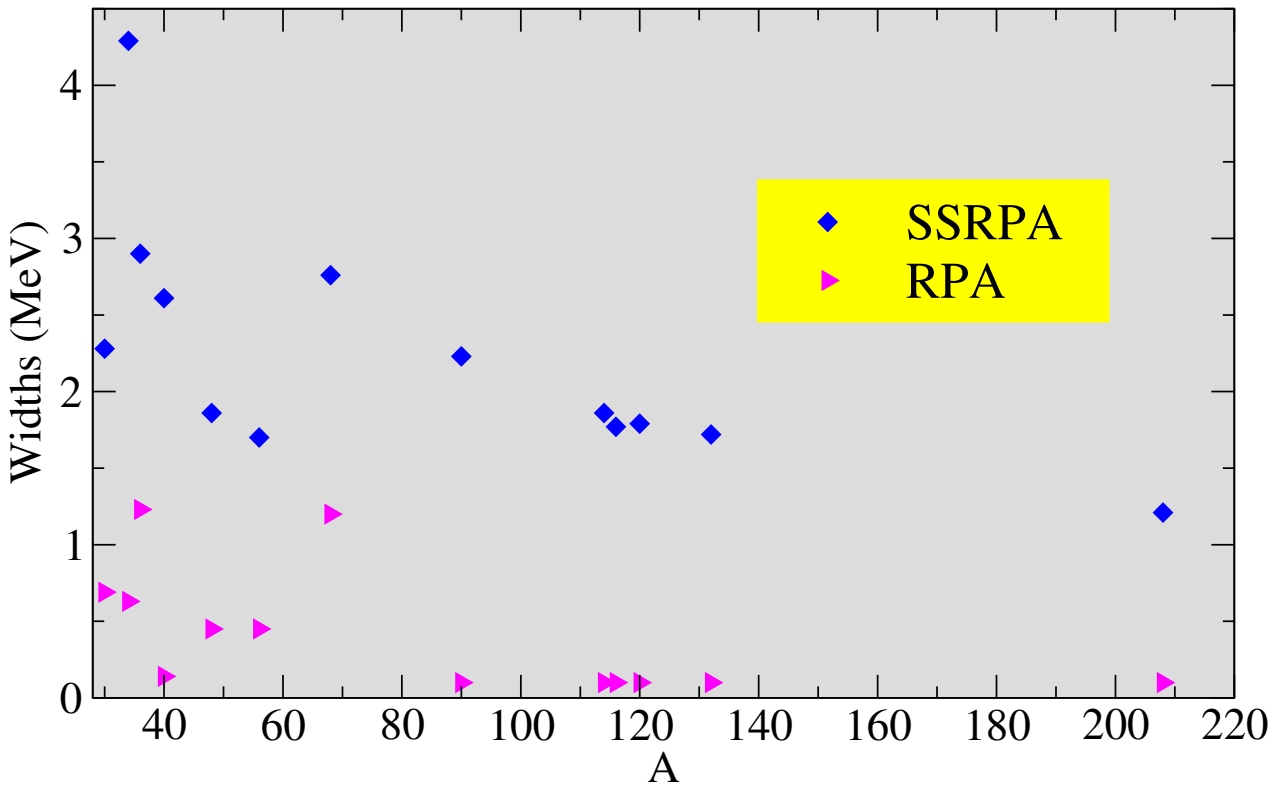

General trend, found both in RPA and in SSRPA: the width is systematically reduced going from lighter to heavier nuclei (Landau damping)
Vasseur, Gambacurta, Grasso, PRC 98, 044313 (2018)

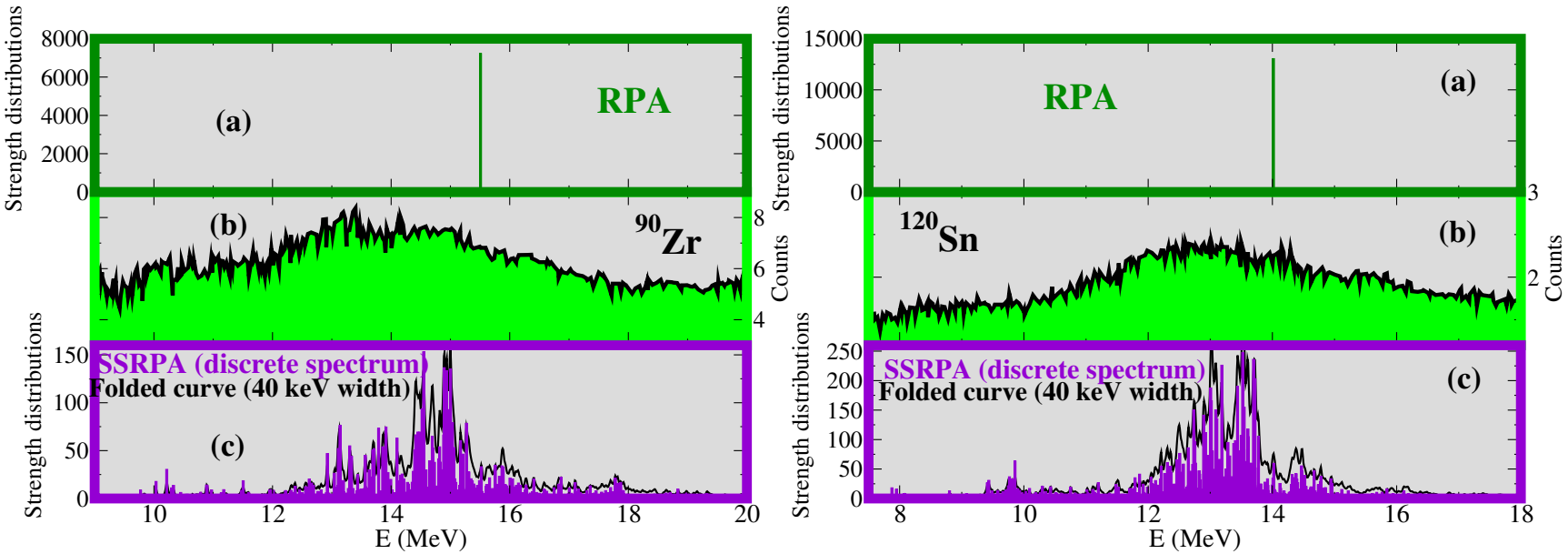

Exp. data: Shevchenko et al, PRL 93, 122501 (2004)

From : Vasseur, Gambacurta, Grasso, PRC 98, 044313 (2018)